Cylindrical β-Sheet Peptide Assemblies

Thomas D. Clark, Jillian M. Buriak,† Kenji Kobayashi,‡ Markus P. Isler, Duncan E. McRee, and M. Reza Ghadiri*

Contribution from the Departments of Chemistry and Molecular Biology and the Skaggs Institute for Chemical Biology, The Scripps Research Institute, La Jolla, California 92037

Received April 30, 1998

Abstract: Recent reports have shown that cyclic peptides composed of an even number of alternating D- and L-amino acids can adopt flat, disklike conformations and stack through backbone−backbone hydrogen-bonding to form extended nanotubular structures. The present work details a general strategy for limiting this self-assembly process through backbone alkylation, giving rise to cylindrical β-sheet peptide dimers. Scope and limitations of dimerization are examined through NMR, FT-IR, mass spectral, and X-ray crystallographic studies of 20 cyclic peptides varying in ring size, location and identity of backbone alkyl substituents, and amino acid composition. The cyclic peptides are shown to self-assemble both in solution and in the solid state through the expected antiparallel β-sheet hydrogen-bonding network. While solution dimerization by cyclic octapeptides appears general, peptides with alternative smaller or larger ring sizes fail to self-associate. Formation of cylindrical β-sheet ensembles is found to tolerate a number of backbone *N*-alkyl substituents, including methyl, allyl, *n*-propyl, and pent-4-en-1-yl groups, as well as a range of amino acid side chains. Within the hemi-*N*-methylated octapeptide framework, residues exhibit differential propensities for dimer stabilization, analogous to amino acid β-sheet propensities in natural systems. Dimer-forming cyclic D,L-peptides are thus among the most structurally well characterized and synthetically accessible β-sheet peptide model systems.

Introduction

Hollow tubular structures with nanometer-sized interiors are well precedented in both natural and artificial systems. Tobacco mosaic virus[1] and transmembrane channel proteins[2] are examples of biological nanotubes, while mesoporous aluminosilicates[3] and graphite nanotubes[4] belong to the synthetic realm. Recent reports from this laboratory have described a convergent approach to design and construction of biomaterial-based nanotubular structures. Cyclic peptide subunits composed of an even number of alternating D- and L-amino acids (cyclic D,L-peptides) were designed to adopt flat, ring-shaped conformations and self-assemble through a β-sheetlike hydrogen-bonding pattern (Figure 1a).[5] The resulting peptide nanotubes have been characterized both in the solid state and in lipid bilayers and in the latter case have been shown to form transmembrane channels capable of transporting ions and small molecules.[6] To study thermodynamic and structural underpinnings of these self-assembly processes in greater detail, truncated peptide nanocylinders were prepared through selective incorporation of *N*-methylated residues, thereby limiting self-assembly to formation of hydrogen-bonded dimers (Figure 1b).[7] The present study explores scope and limitations of this mode of self-assembly in 20 cyclic peptides varying in ring size, backbone alkylation, and amino acid composition.

Design Principles

Self-Assembling Cyclic D,L-Peptide Nanotubes. In 1974, within the context of a theoretical analysis of cylindrical β-helical conformations accessible to linear D,L-peptides, De Santis *et al.* recognized the possibility of forming related cylindrical structures by ring-stacking of heterochiral *cyclic* peptides.[8,9] Early attempts by Lorenzi and co-workers to experimentally verify these predictions met with limited success, partially due to extreme insolubility of the peptides examined.[10a,b] In 1993, electron microscopy, electron diffraction, FT-IR, and molecular modeling studies carried out in this laboratory provided the first compelling evidence of hollow tubular structures formed by self-assembling cyclic D,L-peptides.[5a] This and subsequent reports have shown that cyclic D,L-peptides can

† Present address: 1393 Brown Laboratories, Department of Chemistry, Purdue University, West Lafayette, IN 47907-1393.

‡ Present address: Department of Chemistry, University of Tsukuba, Tsukaba, 305-8571, Japan.

(1) Namba, K.; Stubbs, G. *Science* **1986**, *231*, 1401−1406.

(2) (a) Doyle, D. A.; Cabral, J. M.; Pfuetzner, R. A.; Kuo, A.; Gulbis, J. M.; Cohen, S. L.; Chait, B. T.; Mackinnon, R. *Science* **1998**, *280*, 69−77. (b) Eisenberg, B. *Acc. Chem. Res.* **1998**, *31*, 117−123.

(3) (a) Wu, C.-G.; Bein, T. *Science* **1994**, *264*, 1757−1759. (b) Kresge, C. T.; Leonowicz, M. E.; Roth, W. J.; Vartuli, J. C.; Beck, J. S. *Nature* **1992**, *359*, 710−712.

(4) (a) Iijima, S. *Nature* **1991**, *354*, 56−58. (b) Ajayan, P. M.; Ebbeson, T. W. *Rep. Prog. Phys.* **1997**, *60*, 1025−1062.

(5) (a) Ghadiri, M. R.; Granja, J. R.; Milligan, R. A.; McRee, D. E.; Khazanovich, N. *Nature* **1993**, *366*, 324−327. (b) Khazanovich, N.; Granja, J. R.; McRee, D. E.; Milligan, R. A.; Ghadiri, M. R. *J. Am. Chem. Soc.* **1994**, *116*, 6011−6012. (c) Hartgerink, J. D.; Granja, J. R.; Milligan, R. A. Ghadiri, M. R. *J. Am. Chem. Soc.* **1996**, *118*, 43−50.

(6) (a) Ghadiri, M. R.; Granja, J. R.; Buehler, L. K. *Nature* **1994**, *369*, 301−304. (b) Granja, J. R.; Ghadiri, M. R. *J. Am. Chem. Soc.* **1994**, *116*, 10785−10786. (c) Engels, M.; Bashford, D.; Ghadiri, M. R. *J. Am. Chem. Soc.* **1995**, *117*, 9151−9158. (d) Moteshari, K.; Ghadiri, M. R. *J. Am. Chem. Soc.* **1997**, *119*, 11306−11312. (e) Kim, H. S.; Hartgerink, J. D.; Ghadiri, M. R. *J. Am. Chem. Soc.* **1998**, *120*, 4417−4424.

(7) (a) Ghadiri, M. R.; Kobayashi, K.; Granja, J. R.; Chadha, R. K.; McRee, D. E. *Angew. Chem., Int. Ed. Engl.* **1995**, *34*, 93−95. (b) Kobayashi, K.; Granja, J. R.; Ghadiri, M. R. *Angew. Chem., Int. Ed. Engl.* **1995**, *34*, 95−98. (c) Clark, T. D.; Ghadiri, M. R. *J. Am. Chem. Soc.* **1995**, *117*, 12364−12365.

(8) De Santis, P.; Morosetti, S.; Rizzo, R. *Macromolecules* **1974**, *7*, 52−58.

S0002-7863(98)01485-1 CCC: $15.00
Published on Web 08/19/1998

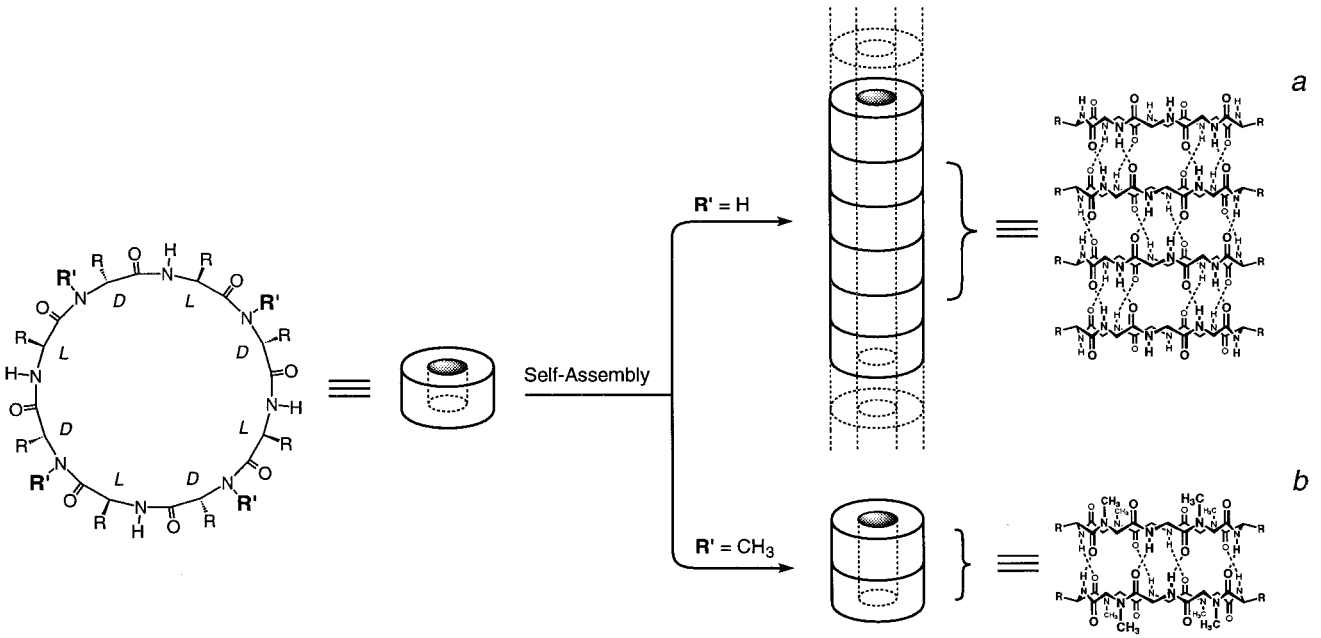

Figure 1. Self-assembling cyclic D,L-peptide nanotubes. Subunits are designed to adopt flat, disklike conformations and stack through antiparallel β-sheet backbone−backbone hydrogen-bonding. (a) All backbone amide groups are free to participate in intermolecular hydrogen-bonding, resulting in extended nanotubular arrays. (b) One face of the peptide ring is *N*-methylated, giving rise to dimeric peptide nanocylinders. (For clarity, most side chains are omitted.)

adopt flat, ring-shaped conformations in which backbone amide groups lie nearly perpendicular to the plane of the peptide ring, while amino acid side chains occupy equatorial positions along the ring's edge.[5−7,10c,d,11] These conformational features leave backbone functionalities of each subunit unhindered and free to hydrogen bond with other like molecules, giving rise to elongated tubular arrays through an extended β-sheet hydrogen-bonding network (Figure 1a). In principle, these β-sheet structures could exist in either parallel or antiparallel orientations, or even as a mixture of the two. However, both computational[12] and experimental[7b] findings demonstrate a thermodynamic preference for the antiparallel arrangement (*vide infra*).

Nanocylinders from Cyclic D,L-Peptides. Due to the highly cooperative nature of nanotube assembly, cyclic D,L-peptides are often extremely insoluble and readily precipitate to form microcrystalline aggregates unsuitable for X-ray crystallographic analysis.[5−7] Modeling studies indicated that introduction of backbone *N*-methyl substituents at alternating residues would render one face of the peptide ring incapable of participating in intersubunit hydrogen-bonding, thereby increasing solubility and limiting self-association to formation of dimeric peptide nanocylinders (Figure 1b). Indeed, peptide *cyclo*[(-L-Phe-D-^{Me}*N*-Ala)$_4$-] (**1**) displays good solubility in nonpolar solvents such as chloroform and dichloromethane. In contrast, non-*N*-alkylated cyclic D,L-peptides are generally soluble only in polar organic solvents (*e.g.*, dimethyl sulfoxide (DMSO) or trifluoroacetic acid (TFA)), which compete effectively for intermolecular hydrogen-bonding sites.[5,6a,b] The hydrophobic sequence of **1** was chosen to confer solubility in apolar media, which both enhance intersubunit hydrogen-bonding and provide a model environment for study of nanotube transmembrane ion channels recently reported from this laboratory.[6]

Octapeptide **1** has been shown to dimerize both in solution and in the solid state through the expected antiparallel β-sheet hydrogen-bonding pattern (Figure 2).[7a] In related work, Lorenzi *et al.* have reported analogous dimerization by hexapeptides *cyclo*[(-D-Leu-L-^{Me}*N*-Leu)$_3$-] and *cyclo*[(-D-Leu-L-Leu)$_2$-D-Leu-L-^{Me}*N*-Leu-].[10c,d] Furthermore, a recent report from this laboratory demonstrated that racemic mixtures of **1** and its enantiomer (*ent*-**1**) self-assemble into both homodimeric antiparallel (**1**·**1** + *ent*-**1**·*ent*-**1**) as well as heterodimeric parallel (**1**·*ent*-**1**) β-sheet structures.[7b] Measurement of solution equilibrium constants revealed that the antiparallel orientation is favored over parallel by 0.8 kcal mol^{-1}. Recent computational studies corroborate these findings.[12b]

Scope of Study

Cyclic Peptide Ring Size. The design strategy outlined above, in principle, allows facile adjustment of nanotube pore dimensions by varying the cyclic peptide ring size.[13] Early modeling results indicated that subunits composed of eight alternating D- and L-amino acid residues would display optimal

(9) In related work, Hassall proposed in 1972 that cyclic tetrapeptides composed of alternating α- and β-amino acids would stack through backbone−backbone hydrogen-bonding to form hollow tubular structures. (a) Hassall, C. H. In *Chemistry and Biology of Peptides: Proceedings of the Third American Peptide Symposium*; Meienhoffer, J., Ed.; Ann Arbor Sci.: Ann Arbor, MI, 1972; pp 153−157. Later, X-ray crystallographic studies only partially validated these predictions. (b) Karle, I. L.; Handa, B. K.; Hassall, C. H. *Acta Crystallogr.* **1975**, *B31*, 555−560. For subsequent reports of self-assembling nanotube structures based on cyclic β^3-peptides, see: (c) Seebach, D.; Matthews, J.; Meden, A.; Wessels, T.; Baerlocher, C.; McCusker, L. B. *Helv. Chim. Acta* **1997**, *80*, 173−182. (d) Clark, T. D.; Buehler, L. K.; Ghadiri, M. R. *J. Am. Chem. Soc.* **1998**, *120*, 651−656.

(10) (a) Tomasi, L.; Lorenzi, G. P. *Helv. Chim. Acta* **1987**, *70*, 1012−1016. (b) Pavone, V.; Benedetti, E.; Di Blasio, B.; Lombardi, A.; Pedone, C.; Lorenzi, G. P. *Biopolymers* **1993**, *28*, 215−223. (c) Saviano, M.; Lombardi, A.; Pedone, C.; Di Blasio, B.; Sun, X. C.; Lorenzi, G. P. *J. Incl. Phenom.* **1994**, *18*, 27−36. (d) Sun, X. C.; Lorenzi, G. P. *Helv. Chim. Acta* **1994**, *77*, 1520−1526.

(11) For recent reports from other laboratories concerning self-assembling cyclic D,L-peptide nanotubes, see: (a) Karlströem, A.; Udén, A. *Biopolymers* **1997**, *41*, 1−4. (b) Carloni, P.; Andreoni, W.; Parrinello, M. *Phys. Rev. Lett.* **1997**, *79*, 761−764. (c) Fukasaku, K.; Takeda, K.; Shiraishi, K. *J. Phys. Soc. Jpn.* **1997**, *66*, 3387−3390. (d) Lewis, J. P.; Pawley, N. H.; Sankey, O. F. *J. Phys. Chem.* **1997**, *101*, 10576−10583.

(12) (a) Chou, K.-C.; Pottle, M.; Nemethy, G.; Ueda, Y.; Scheraga, H. A. *J. Mol. Biol.* **1982**, *162*, 89−112. (b) Gailer, C.; Feigel, M. *J. Comput.-Aided Mol. Des.* **1997**, *11*, 273−277.

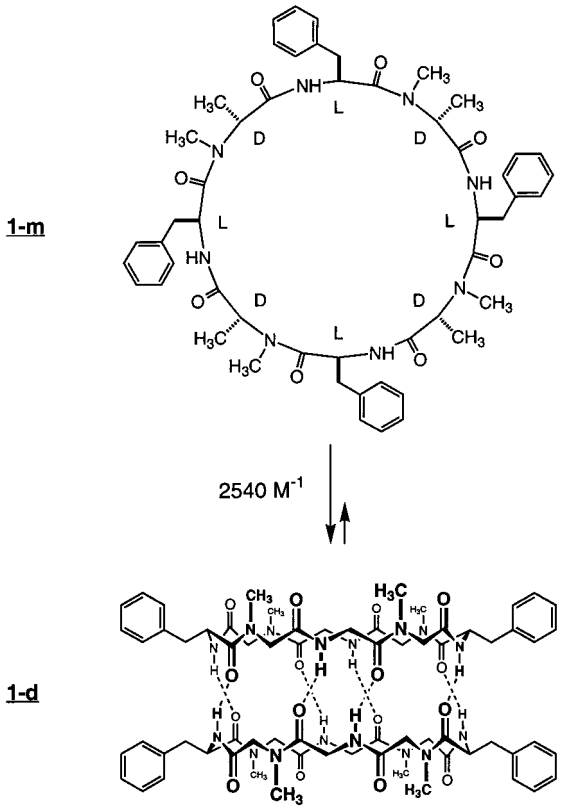

Figure 2. As an illustrative example, *cyclo*[(-L-Phe-D-^{Me}*N*-Ala)$_4$-] (**1**) self-assembles in anhydrous deuteriochloroform with an association constant of 2540 M^{-1}, giving rise to a single dimeric species detectable by ^{1}H NMR. Monomer **1-m** possesses C_4 symmetry, while dimer **1-d** is D_4 symmetrical. (For clarity, most side chains are omitted.)

structural rigidity and predisposition toward nanotube self-assembly. Cyclic hexa-, deca-, and dodecapeptides were also selected for investigation, while smaller cyclic tetrapeptides were found to be incapable of adopting conformations required for intersubunit hydrogen-bonding. Our inaugural study[5a] describing self-assembly of cyclic D,L-octapeptides was followed by subsequent reports of nanotube formation by cyclic deca-[6b] and dodecapeptides.[5b] *N*-Alkylated dimer-forming cyclic octapeptides were also prepared,[7] while Lorenzi *et al.* have reported analogous dimerization by related cyclic hexapeptides.[10c,d] Herein we expand upon these earlier studies to explore hemi-*N*-alkylated subunits with varying ring sizes, including cyclic tetra-, hexa-, octa-, deca-, and dodecapeptides.

Location and Identity of Backbone Alkyl Substituents. Initial reports concerning dimer-forming cyclic peptides focused on compounds whose amide backbone had been partially *N*-methylated.[7,10c,d] The present study expands upon these results by investigating influence of number, position, and identity of backbone *N*-alkyl groups upon the self-assembly process. In addition, modeling studies suggested that introduction of methyl substituents at axial α-positions of every second residue would provide an alternative means of sterically blocking one face of the peptide ring. Thus, the effect of α,α-dialkylated residues is also examined.

Amino Acid Composition. Like that of natural peptide and protein secondary structures, the stability of cyclic D,L-peptide dimers is expected to be influenced by the identity of amino acid side chains. Herein we report initial findings regarding the effect of residue composition on solution dimerization in the hemi-*N*-methylated cyclic octapeptide series.

Table 1. Summary of Cyclic Peptide Dimerization Data

peptide[a,b]	no. of species[c]	K_a (M^{-1})[d]
1 *cyclo*[(-L-Phe^1-D-^{Me}*N*-Ala^2)$_4$-]	2	2540
2 *cyclo*[(-D-Phe^1-L-^{All}*N*-Ala^2)$_4$-]	2	2660
3 *cyclo*[(-D-Phe^1-L-^{Pr}*N*-Ala^2)$_4$-]	2	530
4 *cyclo*[(-D-Phe^1-L-^{All}*N*-Ala^2-D-Phe^3-L-Ala^4)$_2$-]	3	25
5 *cyclo*[(-D-Phe^1-L-^{Pr}*N*-Ala^2-D-Phe^3-L-Ala^4)$_2$-]	3	650
6 *bicyclo*[(-D-Phe^1-L-*N*-(dithiopropyl)-Ala^2-D-Phe^3-L-Ala^4)$_2$-]	2	17
7 *cyclo*[(-D-Phe^1-L-^{Pen}*N*-Ala^2-D-Phe^3-L-Hag^4)$_2$-]	3	920
8 *cyclo*[(D-Phe^1-L-^{Pen}*N*-Ala^2-D-Phe^3-L-^{Me}*N*-Hag^4)$_2$-]	4	440
9 *cyclo*[(-L-Phe^1-D-^{Me}*N*-Ala^2-L-Leu^3-D-^{Me}*N*-Ala^4)$_2$-]	3	800[e]
10 *cyclo*[(-L-Phe^1-D-^{Me}*N*-Ala^2-L-Hag^3-D-^{Me}*N*-Ala^4)$_2$-]	3	100
11 *cyclo*[(-L-Phe^1-D-^{Me}*N*-Ala^2-L-Ile^3-D-^{Me}*N*-Ala^4)$_2$-]	3	28
12 *cyclo*[(L-Phe^1-D-^{Me}*N*-Ala^2-L-Val^3-D-^{Me}*N*-Ala^4)$_2$-]	3	12
13 *cyclo*[(-L-Phe^1-Sar^2)$_4$-]	m	–
14 *cyclo*[(-D-Phe^1-L-^{All}*N*-Ala^2)$_2$-]	1	–
15 *cyclo*[(-L-Phe^1-D-^{Me}*N*-Ala^2)$_3$-]	1	–
16 *cyclo*[(-L-Phe^1-D-^{Me}*N*-Ala^2)$_5$-]	1	–
17 *cyclo*[(-L-Phe^1-D-^{Me}*N*-Ala^2)$_6$-]	m	–
18 *cyclo*[(-L-^{Me}*N*-Phe^1-D-Ala^2)$_4$-]	1	–
19 *cyclo*[(-L-Phe^1-Aib^2)$_4$-]	m	–
20 *cyclo*[(-D-α-Me-Phe^1-L-Ala^2)$_4$-]	1	–

[a] In addition to standard three-letter notations for commonly occurring amino acids, the following abbreviations are used: All = allyl (prop-2-en-1-yl); Pr = *n*-propyl; Pen = (pent-4-en-1-yl); and Hag = homoallylglycine (2-aminohex-5-enoic acid). [b] Superscripts refer to numbering of residues in the peptide ring. [c] Number of interconverting species observed in ROESY experiments (293 K, $CDCl_3$). [d] Association constants determined from variable concentration ^{1}H NMR experiments (293 K, $CDCl_3$) assuming a two-state monomer−dimer equilibrium; a dash (−) appears for entries where no evidence of dimer formation was detected. [e] The association constant of **9** was estimated from a single-point determination.

Results and Discussion

Table 1 summarizes results from investigation of 20 cyclic peptides varying in ring size, location and identity of backbone alkyl substituents, and amino acid composition (superscripts refer to arbitrary numbering of residues; *e.g.*, Phe^1). Peptides were synthesized and purified using standard techniques and subjected to NMR, FT-IR, and mass spectral analysis. Due to conformational averaging on the NMR time scale, ^{1}H NMR spectra of peptides with C_n sequence symmetry (n = 2, 4) are generally C_n and D_n symmetrical for monomeric and dimeric species, respectively. For example, spectra of monomeric octapeptides display resonances corresponding to (1/n)8 residues; likewise, due to mutually perpendicular C_n and C_2 axes, spectra of the corresponding D_n symmetrical dimers show signals corresponding to (1/2n)16 residues. Resonances were assigned from double-quantum-filtered 2D COSY (2QF-COSY)[14] and/or ROESY[15] spectra (see Experimental Section). In all cases, assignments were consistent with both the covalent structure and solution self-association behavior of each peptide. Additionally, four peptides studied gave X-ray diffraction quality crystals, and their solid-state structures are described below.

(13) (a) Cyclic D,L-octa-, deca-, and dodecapeptide nanotubes should display van der Waals internal pore diameters of ∼7, ∼10, and ∼13 Å, respectively. Based on Connolly surface-type calculations using the program HOLE, Smart *et al.*[13b] recently reported an internal radius of 2.48 Å for the tubular transmembrane channel formed by octapeptide *cyclo*[-(L-Trp-D-Leu)$_3$-L-Gln-D-Leu-].[6a] (b) Smart, O. S.; Breed, J.; Smith, G. R.; Sanson, M. S. P. *Biophys. J.* **1997**, *72*, 1109−1126.

(14) Rance, M.; Sørensen, O.; Bodenhausen, G.; Wagner, G.; Ernst, R. R.; Wüthrich, K. *Biochem. Biophys. Res. Commun.* **1983**, *117*, 479−485.

(15) Bothner-By, A. A.; Stephens, R. L.; Lee, J.; Warren, C. D.; Jeanloz, R. W. *J. Am. Chem. Soc.* **1984**, *106*, 811−813.

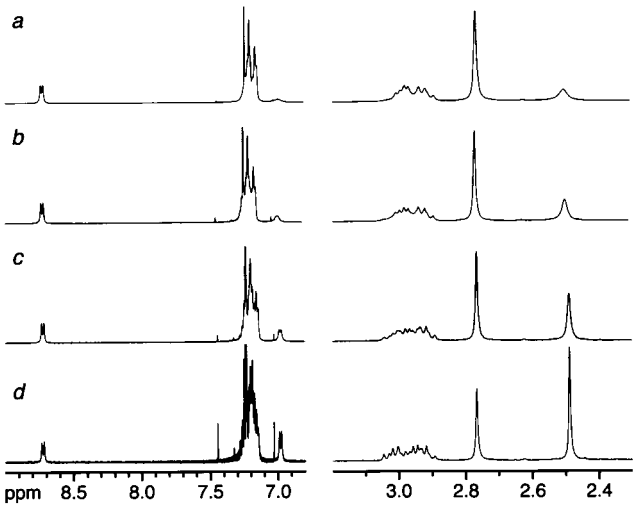

Figure 3. Variable-concentration ^{1}H NMR spectra of peptide **1** showing the following regions: (left) Phe N−H and aromatic and (right) Ala N−CH_3 and Phe C$^\beta$H$_2$ (500 MHz, 293 K, $CDCl_3$). From top to bottom, spectra are arranged in order of diminishing peptide concentration: (a) 4.44, (b) 2.04, (c) 1.07, and (d) 0.44 mM. Due to slow exchange, signals from both monomer (**m**) and dimer (**d**) are observed. As total peptide concentration is lowered, the signal of non-hydrogen-bonded Phe-**m** N−H (6.98 ppm) increases at the expense of the hydrogen-bonded Phe-**d** N−H resonance (8.73 ppm). Likewise, the Ala-**m** N−CH_3 signal (2.49 ppm) increases, while the Ala-**d** N−CH_3 resonance (2.77 ppm) decreases.

Spectral Characterization of Dimer-Forming Cyclic Peptides. In polar solvents such as deuterated methanol or dimethyl sulfoxide, ^{1}H NMR spectra of *cyclo*[(-L-Phe-D-^{Me}*N*-Ala)$_4$-] (**1**) display several slowly interconverting conformers, presumably resulting from *cis*−*trans* isomerization about tertiary amide bonds. From variable-temperature NMR data, the activation barrier for *cis*−*trans* isomerization in DMSO d_6 was estimated to be 16−17 kcal mol^{-1} at the coalescence temperature of 358 K. However, in nonpolar solvents such as deuteriochloroform, **1** exhibits a greatly simplified spectrum due to uniformly *trans* tertiary amide bonds (Figure 3). ROESY spectra ($CDCl_3$) of fourfold symmetrical peptides **1**, **2**, and **3** reveal two species exchanging slowly on the NMR time scale.[16] This slow exchange was unexpected and likely reflects a high activation barrier for concerted breaking of eight hydrogen bonds. In contrast, Lorenzi and co-workers found that dimeric and monomeric forms of hexapeptides *cyclo*[(-D-Leu-L-^{Me}*N*-Leu)$_3$-] and *cyclo*[(-D-Leu-L-Leu)$_2$-D-Leu-L-^{Me}*N*-Leu-] display fast exchange.[10c] Additionally, several twofold symmetrical peptides were examined. In principle, such compounds can dimerize to form two nonequivalent complexes (**d** and **d***), differing in cross-strand pairwise relationships between constituent residues; thus, observation of three slowly interconverting species in ^{1}H NMR spectra was taken as strong evidence of dimer formation (Figure 4, Table 1).[7b,c]

All dimer-forming peptides exhibit concentration-dependent ^{1}H NMR spectra (Figure 3). For example, as total concentration of peptide **1** is decreased, the mole fraction of one species increases at the expense of the other, consistent with an equilibrium between monomer (**m**) and dimer (**d**). Dimer N−H signals are significantly downfield shifted (∼1.7 ppm) relative to those of monomer, indicating tight hydrogen-bonding (Table 2). In contrast, N−H signals of residues not expected to participate in intersubunit hydrogen-bonding (*e.g.*, L-Ala^4 N−H of **4** and **5**) are relatively unchanged upon dimer formation. Additionally, dimer $^3J_{N\alpha}$ values are substantially greater than those of monomers, consistent with the anticipated increase in β-sheet character upon dimer formation. From the parametrized Karplus equation,[17] possible phenylalanine ϕ angles of −120° and −140° were calculated from the $^3J_{N\alpha}$ constants of ∼8.8 Hz observed for dimeric species of peptides **1**−**3**. Furthermore, Phe $^3J_{N\alpha}$ values near 7 Hz for monomers **1-m** and **2-m** suggest

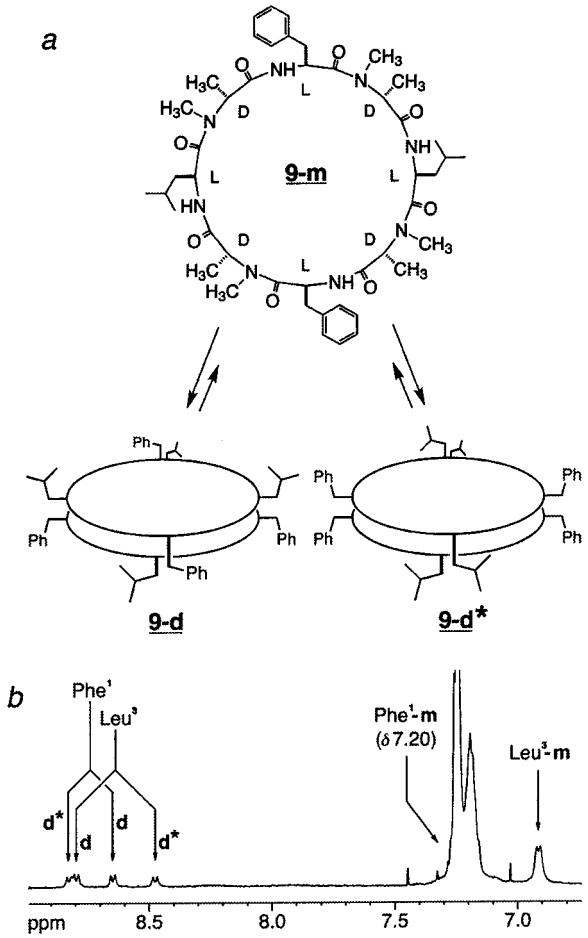

Figure 4. (a) Schematic representation of self-assembly by twofold symmetrical peptide *cyclo*[(-L-Phe-D-^{Me}*N*-Ala-L-Leu-D-^{Me}*N*-Ala)$_2$-] (**9**) to give two nonequivalent dimeric species, **9-d** and **9-d***, which differ in cross-strand pairwise relationships between constituent residues. Monomer **9-m** is C_2 symmetrical, while both **9-d** and **9-d*** possess D_2 symmetry. (b) N−H and aromatic region of the 1D ^{1}H NMR spectrum of **9** (500 MHz, 293 K, 1.5 mM, $CDCl_3$), showing N−H resonances arising from monomer (**m**) as well as the two dimers (**d** and **d***).

Table 2. Summary of NMR Data for Selected Peptides

	Phe $^3J_{N\alpha}$ (Hz)[a]		$\Delta\delta$ (ppm)[b]		
peptide	**m**	**d**	Phe N-H	Phe C$^\alpha$H	Ala C$^\alpha$H
1	7.5	8.8	1.75	0.42	0.63
2	7.0	8.5	1.92	0.23	0.61
3	br[c]	8.7	1.74	0.30	0.87
17	4.9	–	–	–	–

[a] **m** = monomer; **d** = dimer. [b] Change in chemical shift ($\delta_{\mathbf{d}} - \delta_{\mathbf{m}}$) upon dimer formation. [c] Coupling was not observed due to peak broadness.

(16) For NMR, the transition from slow to fast exchange takes place when $k_{ex} = \pi\Delta\nu/\sqrt{2}$, where $\Delta\nu$ is the frequency difference in hertz between exchanging resonances. Sanders, J. K. M.; Hunter, B. K. *Modern NMR Spectroscopy*; Oxford University Press: Oxford, 1987; p 210.

(17) (a) Pardi, A.; Billeter, M.; Wüthrich, K. *J. Mol. Biol.* **1984**, *180*, 741−751. (b) Cavanagh, J.; Fairbrother, W. J.; Palmer, A. G.; Skelton, N. J. *Protein NMR Spectroscopy: Principles and Practice*; Academic Press: San Diego, 1996.

significant preorganization for β-sheet formation. Although literature reports of random coil Phe $^3J_{N\alpha}$ values also range between 7.1 and 7.5 Hz, these quantities are considerably larger than those of many residues with lower β-sheet propensities (*e.g.*, random coil Ala $^3J_{N\alpha}$ = 5.8−6.1 Hz) and suggest persistence of Phe β-strand φ angles even in disordered peptides.[18] By contrast, the Phe $^3J_{N\alpha}$ constant of dodecapeptide **17** (4.9 Hz) is significantly smaller than those of **1-m** and **2-m**, denoting lower intrinsic β-sheet character in **17**, which is consistent with lack of dimerization observed for this peptide.

Additional ^{1}H NMR data support formation of dimeric β-sheet structures. Substantial downfield shifts (>0.1 ppm) in C$^\alpha$H resonances with respect to random coil values are reliable indicators of β-structure.[19] However, literature values for random coil C$^\alpha$H chemical shifts in deuteriochloroform are not available; therefore, we have used the quantity $\Delta\delta = \delta_{dimer} - \delta_{monomer}$ rather than $\Delta\delta = \delta_{folded} - \delta_{random\ coil}$ as is typically employed for peptide and protein structures in water.[20] Thus, downfield shifts observed for dimer C$^\alpha$H resonances with respect to those of monomer are in agreement with dimerization-induced β-sheet formation (Table 2, Figure 5).[21] Furthermore, observation of intense sequential $d_{\alpha-N}$ (i, $i+1$) dimer ROEs is consistent with close spatial proximity of consecutive C$^\alpha$H and N−H protons in a β-strand (data not shown).[22] Finally, as illustrated in Figures 6 and 7, strong cross-strand $d_{\alpha-\alpha}$ ROEs observed for several twofold symmetrical peptides provided compelling evidence of dimeric antiparallel β-sheet structures.[22] ROESY experiments also allowed ^{1}H NMR resonances to be assigned to each of the two expected dimeric species (Figures 6 and 7). Dimers with equivalent non-hydrogen-bonded cross-strand amino acid pairs are designated **d**, while the alternative species are labeled **d***.

Solution ($CHCl_3$) FT-IR studies furnished additional evidence of self-assembled β-sheet structures (Table 3). Amide $I_\perp$ (~1630 cm^{-1})[23] and amide $II_\parallel$ (~1525 cm^{-1}) bands of dimer-forming peptides **1**, **3**, and **10** are characteristic of β-sheets[24] and are similar to those displayed by extended nanotubes formed by non-backbone-alkylated cyclic D,L-peptides.[5,6a,b,d,e] Furthermore, amide A bands appear near 3309 cm^{-1} and indicate hydrogen-bonding. The latter are also in close agreement with amide A values reported by Lorenzi *et al.* for hexapeptide *cyclo*[(-D-Leu-L-^{Me}*N*-Leu)$_3$-] (monomer = 3360 cm^{-1}, dimer = 3309 cm^{-1}).[10] In contrast, peptides **18**−**20**, which show no evidence of dimer formation in ^{1}H NMR experiments, display prominent non-hydrogen-bonded amide A bands at higher energy (Table 3). Peptides **19** and **20** also show weaker low-energy bands at 3269 and 3279 cm^{-1}, respectively, which presumably arise from intramolecular hydrogen-bonding (*vide infra*) and are absent in the case of those peptides which do form dimers (*e.g.*, **1**, **3**, and **10**). In addition, amide $I_\perp$ bands of **19** and **20** appear at values inconsistent with β-structure.

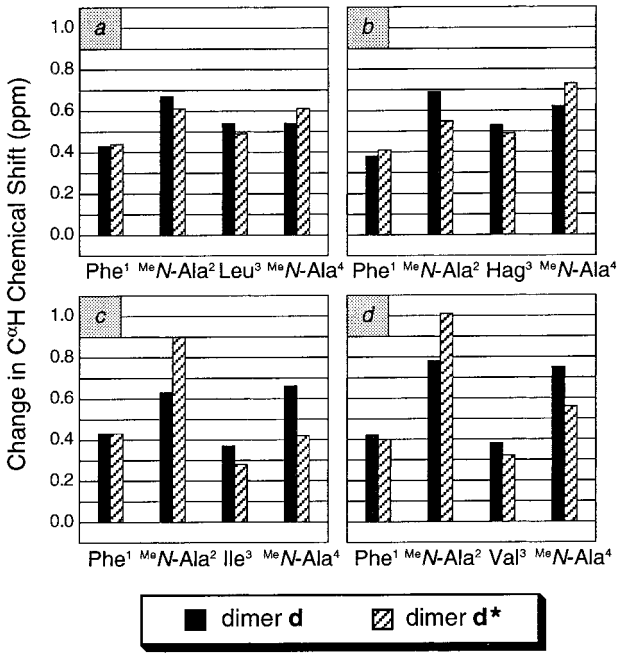

Figure 5. Graphical representation of ^{1}H NMR (500 MHz, $CDCl_3$) C$^\alpha$H chemical shift changes ($\delta_{dimer} - \delta_{monomer}$) for the two nonequivalent dimeric species (**d** and **d***) formed by several twofold symmetrical peptides: (a) *cyclo*[(-L-Phe-D-^{Me}*N*-Ala-L-Leu-D-^{Me}*N*-Ala)$_2$-] (**9**); (b) *cyclo*[(-L-Phe-D-^{Me}*N*-Ala-L-Hag-D-^{Me}*N*-Ala)$_2$-] (**10**); (c) *cyclo*[(-L-Phe-D-^{Me}*N*-Ala-L-Ile-D-^{Me}*N*-Ala)$_2$-] (**11**); and (d) *cyclo*[(-L-Phe-D-^{Me}*N*-Ala-L-Val-D-^{Me}*N*-Ala)$_2$-] (**12**). Observed downfield shifts in dimer signals are consistent with the anticipated increase in β-sheet character upon dimer formation.

Dimer formation was also studied using electrospray ionization mass spectrometry (ESI-MS). Due to its soft ionization conditions, ESI-MS has lately found considerable application in study of noncovalent complexes.[25] We reasoned that the mildness of ESI together with the relatively high K_a of peptide **1** (Table 1) would afford a reasonable chance of detecting dimer **1-d** in the gas phase. Indeed, ESI-MS analysis of **1** revealed singly charged species corresponding to both proton and sodium adducts of **1-d**, strongly supporting solution dimerization by **1** and related compounds (Figure 8).

Thermodynamics of dimer formation were studied by variable-concentration and variable-temperature ^{1}H NMR spectroscopy (*e.g.*, Figure 3). In variable-concentration experiments, the integral ratio (signal from total dimeric species)/(signal from all species) was plotted versus total peptide concentration, and data were fitted to the following equation:[26]

(18) (a) Smith, L. J.; Bolin, K. A.; Schwalbe, H.; MacArthur, M. W.; Thornton, J. M.; Dobson, C. M. *J. Mol. Biol.* **1996**, *255*, 494−506. (b) Serrano, L. *J. Mol. Biol.* **1995**, *254*, 322−333. (c) Swindells, M. B.; MacArthur, M. W.; Thornton, J. M. *Nat. Struct. Biol.* **1995**, *2*, 596−603.

(19) (a) Wishart, D. S.; Sykes, B. D.; Richards, F. M. *Biochemistry* **1992**, *31*, 1647−1651. (b) Wishart, D. S.; Sykes, B. D.; Richards, F. M. *J. Mol. Biol.* **1991**, *222*, 311−333. (c) Williamson, M. P. *Biopolymers* **1990**, *29*, 1423−1431.

(20) Recent examples of C$^\alpha$H chemical shift analysis in aqueous β-hairpin model systems: (a) Maynard, A. J.; Sharman, G. J.; Searle, M. S. *J. Am. Chem. Soc.* **1998**, *120*, 1996−2007. (b) Haque, T. S.; Gellman, S. H. *J. Am. Chem. Soc.* **1997**, *119*, 2303.

(21) For reasons which remain unclear, C$^\alpha$H resonances of D-Phe^1 in **4** and **7** as well as D-Phe^3 in **5** and **6** experience moderate *upfield* shifts upon dimer formation. However, C$^\alpha$H signals of the other three constituent residues in these peptides display the expected downfield shifts. Additionally, dimer-forming cyclic D,L-octapeptides bearing four *N*-alkyl substituents show anticipated downfield shifts in all C$^\alpha$H resonances (*e.g.*, Figure 5).

(22) *Two Dimensional NMR Spectroscopy: Applications for Chemists and Biochemists*, 2nd ed.; Croasmun, W. R., Carlson, R. M. K., Eds.; VCH: New York, 1994.

(23) For partially *N*-alkylated peptides, an additional strong amide $I_\perp$ band near 1675 cm^{-1} was also observed, presumably arising from non-hydrogen-bonding amide groups (Table 3). Observation of this signal even in the FT-IR spectrum of nondimer-forming peptide **18** suggests that it is not an amide $I_\parallel$ band, which for an antiparallel β-sheet[24] appears as a weak signal near 1694 cm^{-1} and is absent in disordered peptides. Amide $I_\parallel$ bands of dimer-forming peptides likely overlap with amide $I_\perp$ signals of non-hydrogen-bond *N*-alkylated residues.

(24) Bandekar, J. *Biochim. Biophys. Acta* **1992**, *1120*, 123−143.

(25) Siuzdak, G. *Mass Spectrometry for Biotechnology*; Academic Press: San Diego, 1996.

(26) As put forth by Ho and DeGrado, the generalized form of eq 1 can be applied to multimeric assembly and contains a term, n, the aggregation state of the molecule under study. For the present system, we have considered only the specialized case of $n = 2$ (dimerization), which has been shown by NMR, ESI-MS, and X-ray crystallographic evidence to be the most reasonable model for solution self-association. Ho, S. P. H.; DeGrado, W. F. *J. Am. Chem. Soc.* **1987**, *109*, 6751−6758.

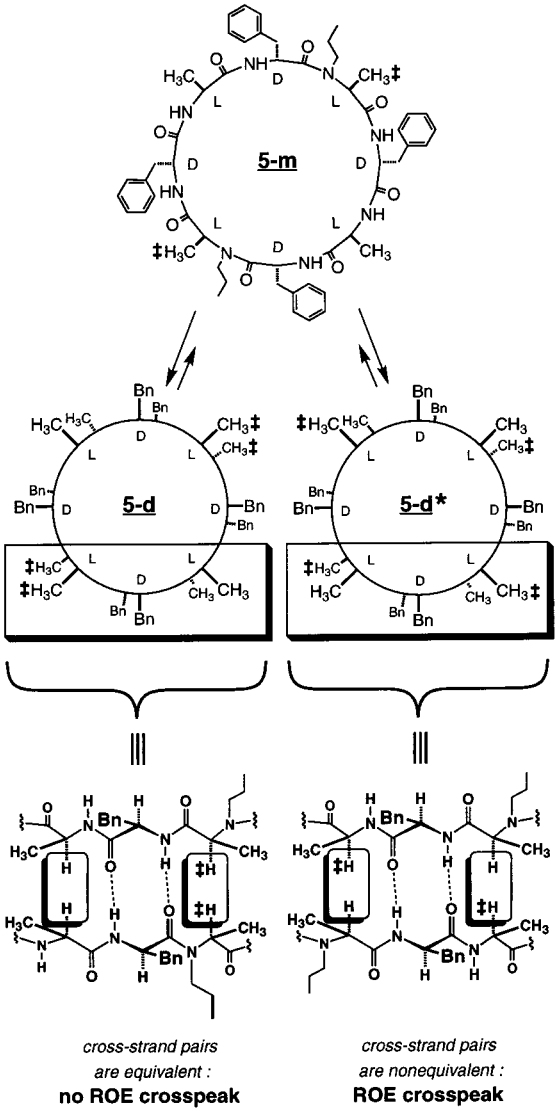

Figure 6. Schematic representation of solution self-assembly by twofold symmetrical peptide *cyclo*[(-D-Phe[1]-L-^{Pr}*N*-Ala[2]-D-Phe[3]-L-Ala[4])$_2$-] (**5**); *N*-propylated Ala[2] residues are marked with a dagger sign (‡) to differentiate them from unsubstituted Ala[4]. Monomer **5-m** self-associates to give two nonequivalent dimeric species, **5-d** and **5-d***, which differ in cross-strand pairwise relationships between constituent residues. **5-d** and **5-d*** can be distinguished using 2D ROESY experiments, since in **5-d*** nonequivalent ^{Pr}*N*-Ala[2] (‡) and Ala[4] C$^{\alpha}$H protons are in close spatial proximity and should, therefore, give rise to $d_{\alpha-\alpha}$ ROE cross-peaks (Figure 7a). Analogous ROE cross-peaks are not expected for either monomer **5-m** or the alternative dimeric complex **5-d**.

$$[\mathrm{P}]_t = \frac{\Delta I_{obs} K_d}{2\Delta I_{sat}(1 - (\Delta I_{obs}/\Delta I_{sat}))^2} \qquad (1)$$

where $[\mathrm{P}]_t$ is total peptide concentration, ΔI_{obs} is the signal intensity from dimeric species divided by total signal intensity, ΔI_{sat} is the expected signal intensity from dimeric species divided by total signal intensity under saturating conditions (*i.e.*, all dimer, no monomer), and K_d is the dissociation constant. In all cases, a simple two-state monomer−dimer equilibrium was assumed in order to allow direct comparison among entries.

Association constants determined for peptide **1** at 298 K are as follows: $K_a(CDCl_3/CCl_4\ 84{:}16) = 1.4 \times 10^4\ M^{-1}$ and $K_a(CDCl_3) = 1.26 \times 10^3\ M^{-1}$.[27] Thus, dimer **1-d** is favored over monomer **1-m** by 4.0−5.6 kcal mol^{-1}, depending on solvent employed. Additionally, under rigorously anhydrous conditions, the association constant for peptide **1** in deuteriochloroform approximately doubles, with $K_a(CDCl_3 + 4$ Å molecular sieves$) = 2.54 \times 10^3\ M^{-1}$ (Table 1), suggesting competition by water for intermolecular hydrogen-bonding sites.

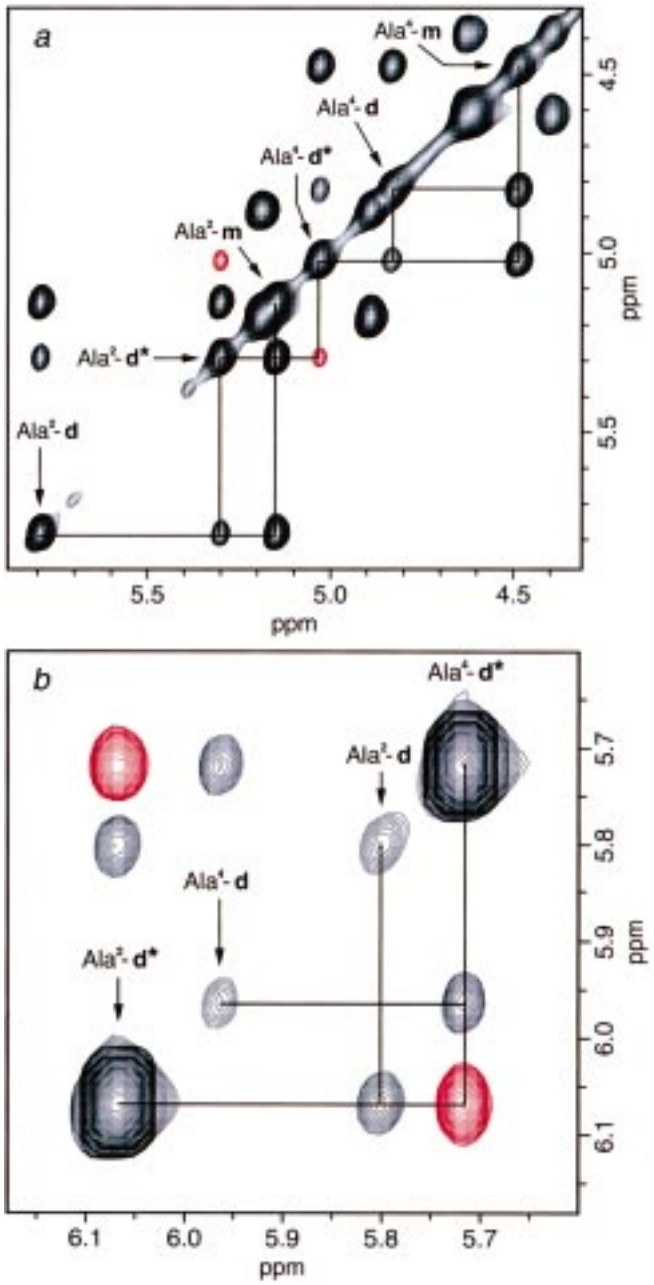

Figure 7. ROESY spectra of selected twofold symmetrical dimer-forming peptides: (a) C$^{\alpha}$H region for *cyclo*[(-D-Phe[1]-L-^{Pr}*N*-Ala[2]-D-Phe[3]-L-Ala[4])$_2$-] (**5**) (400 MHz, 293 K, 2.0 mM, $CDCl_3$); (b) dimer Ala C$^{\alpha}$H region for *cyclo*[(-L-Phe-D-^{Me}*N*-Ala-L-Ile-D-^{Me}*N*-Ala)$_2$-] (**11**) (500 MHz, 293 K, 22.1 mM, $CDCl_3$). Exchange cross-peaks (black) are observed between resonances arising from the monomer (**m** in a) and two dimers (**d** and **d***in a and b). However, only dimers **d*** show ROE cross-peaks (red) between Ala[2] and Ala[4] C$^{\alpha}$H signals due to close spatial proximity of the corresponding protons in these species (Figure 6).

(27) Standard deviations are not reported because many of these dimerization experiments were performed only once. However, in fitting experimental data to eq 1, ΔI_{sat} was treated as a parameter and allowed to vary; thus, comparison of experimental and theoretical values of ΔI_{sat} provides an approximation of error in K_d. On this basis, we estimate the association constants reported in Table 1 to be accurate within ±20%. Additionally, goodness of fit (*R* values) ranged between 0.92 and 0.999.

Table 3. Summary of FT-IR Data for Selected Peptides

peptide	amide A[a]	amide $I_{\perp}$[b]	amide $II_{\parallel}$
1	3309	1628 (1677)	1523
3	3306	1625 (1675)	1525
9	3310	1631 (1675)	1527
18	3343	1644 (1675)	ovl[c]
19	3269 3379	1676	1520
20	3277 3369	1674	1518

[a] Peptides **19** and **20** display both an intramolecularly hydrogen-bonded amide A band (upper value) and a non-hydrogen-bonded band (lower value). [b] Values in parentheses are putative amide $I_{\perp}$ bands arising from non-hydrogen-bonding *N*-alkylated residues. [c] The amide $II_{\parallel}$ band of **18** overlaps with nearby signals.

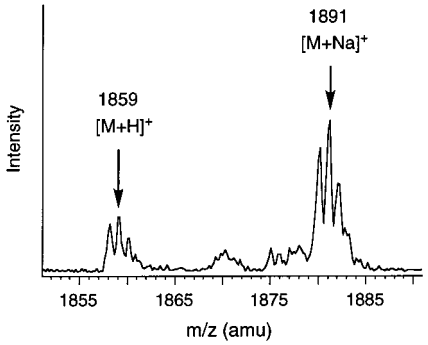

Figure 8. ESI mass spectrum of peptide **1** showing signals arising from noncovalent dimer **1-d** (Figure 2). Both proton (MH^+ calcd = 1859, found = 1859) and sodium (MNa^+ calcd = 1891, found = 1891) adducts are observed; in both cases, the separation of C^{13} isotope peaks (~1 amu) indicates singly charged species.

The observed 2-fold change in K_a of peptide **1** in the presence and absence of small amounts of water represents only a minor energy difference (0.4 kcal mol^{-1}). By analogy to the work of Adrian and Wilcox,[28] water is expected to weaken hydrogen-bonding and diminish binding enthalpy; however, this loss should be largely counterbalanced by favorable entropy changes resulting from release of bound water:

$$2[\mathbf{m}\cdot(H_2O)_n] \rightarrow \mathbf{m}::\mathbf{m}\cdot(H_2O)_{(n-x)} + (H_2O)_x \qquad (2)$$

Variable-temperature ^1H NMR studies (van't Hoff plots) established the following thermodynamic parameters for dimerization of **1** in $CDCl_3$ (no molecular sieves): $\Delta C_p = -203.1$ cal K^{-1} mol^{-1}, $\Delta H°_{298} = -11.0$ kcal mol^{-1}, and $\Delta S°_{298} = -23.7$ cal K^{-1} mol^{-1}. These negative enthalpy and entropy terms, together with the observed inverse relationship between K_a and solvent polarity, clearly support self-assembly by **1** as an enthalpy-driven, entropy-opposed[29] process caused principally by intermolecular hydrogen-bonding.

Relative to other assembly processes involving comparable numbers of hydrogen bonds, dimer-forming cyclic peptides display unexpectedly low association constants (Table 1).[30] Weak dimerization may arise, in part, from steric repulsion between *N*-alkyl groups and carbonyl oxygens of *N*-alkylated residues. Indeed, computational studies have uncovered such destabilizing effects in β-conformations of *N*-alkylated model peptides.[31]

Effect of Cyclic Peptide Ring Size on Solution Dimerization Affinity. The effect of cyclic peptide ring size on solution dimerization affinity was examined in the series *cyclo*[(-L-Phe-D-^{Me}*N*-Ala)$_n$-], where $n = 3-6$ for compounds **15**, **1**, **16**, and **17**, respectively. Cyclic tetramer **14** was also investigated.[32] As expected from modeling results, **14** displays no evidence of self-association in ^1H NMR experiments. Decapeptide **16** and dodecapeptide **17** also fail to self-associate, likely due to greater conformational flexibility and diminished preorganization for self-assembly with respect to octapeptide **1**. Consistent with this interpretation, ^1H NMR spectra of **16** show broad signals, while those of **17** reveal several slowly interconverting conformers. Additionally, the observed Phe $^3J_{N\alpha}$ value of 4.9 Hz indicates little β-sheet character in **17** (Table 2).[17]

Hexapeptide **15** also shows no evidence of self-association in ^1H NMR experiments. This result is surprising in light of reports by Lorenzi *et al.* describing solid-state and/or solution dimerization by partially *N*-methylated hexapeptides *cyclo*-[(-D-Leu-L-^{Me}*N*-Leu)$_3$-] and *cyclo*[(-D-Leu-L-Leu)$_2$-D-Leu-L-^{Me}*N*-Leu-].[10c,d] These results suggest that dimer formation by cyclic hexapeptides is strongly dependent on residue composition.

Effect of Identity and Location of Backbone Alkyl Substituents on Solution Dimerization Affinity. The dimerization process was found to tolerate a variety of amide *N*-alkyl substituents, including methyl, allyl, *n*-propyl, and pent-4-en-1-yl groups (Table 1). Replacement of the four *N*-methyl substituents in parent compound **1** with allyl groups results in no loss of dimerization affinity (entry **2**), while tetra-*N*-(*n*-propyl) derivative **3** suffers only a 5-fold reduction in association constant relative to **1** and **2**.[32] As anticipated from modeling results, two *N*-alkyl substituents also proved sufficient to limit self-assembly to dimer formation (entries **4**−**7**). Unexpectedly, the K_a of di-*N*-allyl peptide **4** is diminished by 2 orders of magnitude relative to both tetra-*N*-allyl derivative **2** and parent peptide **1**, while simple reduction of olefinic functionalities to give di-*N*-(*n*-propyl) compound **5** restores much of the binding affinity. Interestingly, in contrast to other twofold symmetrical peptides which self-associate to form two nonequivalent dimers (Figures 4 and 6), heterodectic bicyclic octapeptide **6**, containing an intramolecular disulfide bridge, gives only one dimeric species. In ^1H NMR spectra of **6**, D-Phe^1 and D-Phe^3 N−H resonances are downfield shifted upon dimerization by only 0.99 and 0.28 ppm, respectively, indicating weaker intersubunit hydrogen-bonding than in other peptides examined (Table 2). We attribute this unusual behavior to deformation of the peptide cycle caused by the intramolecular disulfide bond, simultaneously decreasing dimerization avidity and allowing self-association in only one supramolecular orientation.

Peptides **7** and **8**, bearing larger *N*-(pent-4-en-1-yl) substituents, also show significant dimerization affinity. Unexpectedly, the ROESY spectrum of **8** revealed four slowly interconverting species—the anticipated two dimers as well as two conformational isomers of the monomer, the latter possibly caused by *cis*−*trans* isomerization about tertiary amide bonds. Interestingly, *N*-methylation of Hag residues of **7** to give **8** causes only a 2-fold decrease in the association constant, while ^{Me}*N*-Phe-

(28) (a) Adrian, J., Jr.; Wilcox, C. S. *J. Am. Chem. Soc.* **1991**, *113*, 678−680. (b) Adrian, J., Jr.; Wilcox, C. S. *J. Am. Chem. Soc.* **1992**, *114*, 1398−1403.

(29) (a) Searle, M. S.; Westwell, M. S.; Williams, D. H. *J. Chem. Soc., Perkin Trans. 2* **1995**, 141−151. (b) Dunitz, J. D. *Chem. Biol.* **1995**, *2*, 709−712.

(30) Fredericks, J. R.; Hamilton, A. D. In *Comprehensive Supramolecular Chemistry, Vol. 9*; Sauvage, J.-P., Hosseini, M., Eds.; Elsevier Science Ltd.: Oxford, 1996; pp 565−594.

(31) Möhle, D.; Hofman, H.-J. *J. Pept. Res.* **1998**, *51*, 19−28.

(32) Residues in **1** are enantiomeric to those of peptides **2**−**6**, **14**, and **20**. However, since only homodimerization is examined in this study, association by these peptides may be compared directly.[7b]

containing peptide **18** showed no evidence of dimer formation in the temperature range 215−293 K, as determined by ^{1}H NMR (2.4 mM, $CDCl_3$). Additionally, interaction of **18** with its enantiomer *ent*-**18**, with **1**, and with *ent*-**1** was investigated, and no evidence of heterodimer formation was observed. Lack of self-association by **18** may arise from unfavorable steric interactions between backbone *N*-methyl substituents and side-chain β-phenyl groups of Phe, since analogous interactions in ^{Me}*N*-Hag residues of **8** are likely less severe.

The influence of α,α-dialkylated residues upon dimerization was also investigated. Modeling studies suggested that introduction of axial α-methyl substituents into every second residue would sterically block one face of the cyclic peptide ring and provide an alternative means of controlling self-assembly. Indeed, α,α-disubstituted peptides **19** and **20**[32] exhibit good solubility in apolar organic solvents such as chloroform and dichloromethane, indicating that α-methylation prevents formation of insoluble hydrogen-bonded aggregates. However, ^{1}H NMR experiments showed that these peptides fail to self-associate, likely due to conformational heterogeneity in monomeric subunits. At room temperature and below, **19** exists as a mixture of slowly interconverting conformers, which converge at elevated temperature (≥318 K) to give a single set of ^{1}H NMR signals. Under ambient conditions, the ^{1}H NMR spectrum of **20** displays one set of resonances which grow increasingly broad at lower temperature, suggesting multiple conformations of similar energy separated by small activation barriers. In contrast, spectra of dimer-forming peptides (*e.g.*, **10**) sharpen considerably as the sample is cooled (293→278 K), suggesting a population of similar conformations converging toward a unique structure. Additionally, solution FT-IR spectra of **19** and **20** show only non-hydrogen-bonded and putative intramolecularly hydrogen-bonded amide N−H stretching bands (Table 3). Intramolecular hydrogen-bonding is further supported by ^{1}H NMR spectra of **19** (293 K, $CDCl_3$), which reveal a weak intensity concentration-independent downfield-shifted N−H resonance (data not shown). Modeling studies indicate that steric repulsion between α-methyl groups and carbonyl oxygens of $i-1$ residues likely destabilize β-conformations in **19** and **20**, thereby preventing dimer formation and giving rise to conformational heterogeneity. Indeed, experimental investigations of α,α-dialkylated peptides have demonstrated a distinct preference for helical rather than β-sheet ϕ,ψ angles.[33]

Effect of Amino Acid Composition on Solution Dimerization Affinity. Stable peptide and protein secondary structures exhibit marked sequence preferences thought to arise from a variety of noncovalent factors, including side chain hydrophobic effects,[34] solvent screening,[35] and steric interactions.[36,37] In the present system, solvent effects should be negligible due to the apolar, noncompeting nature of the surrounding medium. Therefore, sequence preferences for dimer formation should reflect sterically driven conformational propensities of constituent residues.

Preliminary results support these expectations. ^{1}H NMR spectra of *cyclo*[(-L-Phe-D-^{Me}*N*-Ala-L-Leu-D-^{Me}*N*-Ala)$_2$-] (**9**) and *cyclo*[(-L-Phe-D-^{Me}*N*-Ala-L-Hag-D-^{Me}*N*-Ala)$_2$-] (**10**) reveal equal populations of the two anticipated dimers (**d** and **d***), indicating negligible cross-strand side chain interactions (Figure 4).[7b,c] NMR, FT-IR, and X-ray crystallographic evidence suggests that intersubunit hydrogen-bonding and, hence, ΔH of dimerization should be similar for **1**, **9**, and **10**. Translational and rotational entropies of dimerization are also expected to be similar.[38] However, association constants of **1** and **9** are significantly higher than that of **10**, suggesting that Phe and Leu are more effective than Hag at preorganizing the cyclic peptide backbone for β-sheet formation (Table 1).[38] Indeed, statistical,[39] computational,[40] and experimental[35a,41,42] studies have shown that Phe and Leu display greater propensity for β-sheet conformations than does Met, the latter being sterically similar to Hag. Therefore, the observed trend in dimerization affinity (**1** > **9** > **10**) may reflect differences in conformational entropy (ΔS_{conf}) related to β-sheet propensities of Phe, Leu, and Hag, respectively. Also consistent with this interpretation, ^{1}H NMR experiments reveal no evidence of dimer formation by **13** in which the four D-^{Me}*N*-Ala residues of parent peptide **1** have been replaced by the more flexible sarcosine (*N*-methylglycine).

We note that energetics of dimerization by **1**, **9**, and **10** are likely influenced by entropies of mixing (ΔS_{mix}). For twofold symmetrical peptides **9** and **10**, ΔS_{mix} should be more favorable than for **1** due to formation of two nonequivalent dimeric species (**d** and **d***, Figure 3). Thus, ΔS_{mix} is expected to *augment* dimer formation by **9** and **10** and should not alter the overall trend in association constants (*i.e.*, **1** > **9** > **10**).

β-Branched residues Ile and Val are known to exhibit high propensities for β-conformations. Therefore, the low association constants of *cyclo*[(-L-Phe-D-^{Me}*N*-Ala-L-Ile-D-^{Me}*N*-Ala)$_2$-] (**11**) and *cyclo*[(-L-Phe-D-^{Me}*N*-Ala-L-Val-D-^{Me}*N*-Ala)$_2$-] (**12**) with respect to peptides **9** and **10** may seem surprising (Table 1). However, in β-structures, side chains of Ile and Val are known to strongly favor t conformations ($\chi_1 \approx 180°$),[43] which in the present system should cause unfavorable steric interactions with $i+1$ Ala *N*-methyl groups and disfavor dimerization-induced β-sheet formation. Additionally, although both **11** and **12** form the two expected dimeric species (**d** and **d***), in both cases the mole fraction of **d*** is approximately 4 times that of **d**, implying unfavorable cross-strand side chain interactions which may further diminish dimerization affinity.

Solid-State Structures of Peptides 1, 2, 3, and 9. Formation of dimeric β-sheet structures was conclusively established using

(33) Toniolo, C.; Crisma, M.; Formaggio, F.; Valle, G.; Cavicchioni, G.; Précigoux, G.; Aubry, A.; Kamphuis, J. *Biopolymers* **1993**, *33*, 1061−1071.

(34) Horowitz, A.; Matthews, J. M.; Fersht, A. *J. Mol. Biol.* **1992**, *227*, 560−568.

(35) (a) Bai, Y.; Englander, S. W. *Proteins: Struct., Funct., Genet.* **1994**, *18*, 262−266. (b) Avbelj, F.; Moult, J. *Biochemistry* **1995**, *34*, 755−764.

(36) (a) Hermans, J.; Anderson, A. G.; Yun, R. H. *Biochemistry* **1992**, *31*, 5646−5653. For related studies which address entropic effects in amino acid secondary structural propensities, see: (b) Creamer, T. P.; Rose, G. D. *Proc. Natl. Acad. Sci. U.S.A.* **1992**, *89*, 5937−5941. (c) Padmanabhan, S.; Baldwin, R. L. *J. Mol. Biol.* **1991**, *219*, 135−137.

(37) Early conformational analyses of backbone torsional preferences in amino acids and peptides: (a) Pauling, L.; Corey, R. B. *Proc. Nat. Acad. Sci U.S.A.* **1951**, *37*, 729−741. (b) Ramachandran, G. N.; Sasisekharan, V. *Adv. Prot. Chem.* **1968**, *23*, 283−438.

(38) Simanek, E. E.; Li, X.; Choi, I. S.; Whitesides, G. M. In *Comprehensive Supramolecular Chemistry, Vol. 9*; Sauvage, J.-P., Hosseini, M., Eds.; Elsevier Science Ltd.: Oxford, 1996; p 605.

(39) (a) Chou, P. Y.; Fasman, G. D. *Biochemistry* **1974**, *13*, 211−222. (b) Muñoz, V.; Serrano, L. *Proteins: Struct., Funct., Genet.* **1994**, *20*, 301−311. (c) Swindells, M. B.; MacArthur, M. W.; Thornton, J. M. *Nat. Struct. Biol.* **1994**, *2*, 596−603.

(40) (a) Finkelstein, A. V. *Protein Eng.* **1995**, *8*, 207−209.

(41) (a) Kim, C. A.; Berg, J. M. *Nature* **1993**, *362*, 267−270. (b) Kim, C. A.; Berg, J. M. *Nat. Struct. Biol.* **1996**, *3*, 940−945. (b) Minor, D. L., Jr.; Kim, P. S. *Nature* **1994**, *367*, 660−663. (c) Minor, D. L., Jr.; Kim, P. S. *Nature* **1994**, *371*, 264−267. (d) Minor, D. L., Jr.; Kim, P. S. *Nature* **1996**, *380*, 730−734. (e) Smith, C. K.; Withka, J. M.; Regan, L. *Biochemistry* **1994**, *33*, 5510−5517. (f) Smith, C. K.; Regan, L. *Science* **1995**, *270*, 980−982.

(42) The studies listed in refs 35a and 41 were carried out in aqueous media; therefore, observed trends in amino acid β-sheet propensites should reflect solvophobic and solvent screening effects in addition to side chain−backbone conformational preferences.

(43) Dunbrack, R. L.; Karplus, M. *Nat. Struct. Biol.* **1994**, *1*, 334−340.

Table 4. Backbone Torsion Angles for Crystal Structures of Peptides **1**−**3**[a]

	Phe			Ala		
peptide	ϕ	ψ	ω	ϕ	ψ	ω
1	−116.4	127.0	170.7	136.0	−133.7	−176.0
2	153.4	−133.1	−175.7	−137.5	119.6	172.9
3	145.5	−128.9	−173.1	−140.3	122.4	174.0

[a] For **9**, the following ranges of backbone torsion angles were observed (ϕ; ψ; ω, respectively): L-Phe[1] (−151.2 to −136.75; 127.8 to 129.1; 173.2 to 177.2); D-^{Me}*N*-Ala[2] (132.5 to 134.0; −147.9 to −137.0; −175.8 to −171.7); L-Leu[3] (−129.0 to −122.6; 133.9 to 140.0; 168.6 to 174.9); D-^{Me}*N*-Ala[4] (126.6 to 136.2; −129.7 to −117.1; −175.8 to −171.9).

X-ray crystallography. X-ray diffraction quality crystals were obtained from dichloromethane solutions of **1**, **2**, **3**, and **9** via vapor-phase equilibration with hexanes (see Experimental Section). Following data collection, the structures were solved using direct methods and refined to reveal that, as expected, all four peptides stack through an antiparallel β-sheet hydrogen-bonding pattern to form hollow cylindrical assemblies (Figure 9).

Compounds **1**−**3** display crystallographic fourfold rotational axes parallel to the *c* axis passing through the center of the peptide ring, and the two peptide subunits are related by a twofold rotation along either the *a* or *b* axis. Peptide **9** crystallized in an unsymmetrical conformation, and its asymmetric unit consists of the entire dimeric structure. The presence of disordered water molecules within the cylindrical cavities likely accounts for the unusually high final *R* factors of these structures (8.87, 10.13, 14.20, and 10.45% for **1**, **2**, **3**, and **9**, respectively) and establishes the expected hydrophilicity of the cyclic peptide interiors. *N*-Methyl groups of compounds of **1** and **9** are oriented nearly perpendicular to the plane of the peptide ring, while longer *N*-allyl and *N*-(*n*-propyl) substituents of **2** and **3**, respectively, curve over and occlude the cylinder pores. In each case, backbone torsion angles (ϕ,ψ,ω) of all residues fall within the β-sheet region of the Ramachandran map (Table 4). All side chains adopt orientations favored by β-structures,[43] with Phe (peptides **1**, **2**, **3**, and **9**) and Leu (peptide **9**) assuming t ($\chi_1 \approx 180°$) and g$^-$ ($\chi_1 \approx -60°$) conformations, respectively.

Summary and Conclusions

In summary, NMR, FT-IR, ESI-MS, and X-ray diffraction data have provided conclusive evidence of dimeric β-sheet structures formed by backbone-alkylated heterochiral cyclic peptides. Partial amide *N*-alkylation has been shown to block peptide aggregation and limit self-assembly to dimer formation. The dimerization process tolerates a number of *N*-alkyl substituents, including methyl, allyl, *n*-propyl, and pent-4-en-1-yl groups. Although no obvious relationship was observed between solution dimerization affinity and number and/or identity of *N*-alkyl substituents, the available data suggest that the location of backbone *N*-alkyl groups can exert a strong effect. Furthermore, α,α-disubstituted peptides **19** and **20** showed no evidence of solution dimerization, reflecting the preference of α,α-dialkylated residues for helical rather than β-sheet conformations.[33] The effect of cyclic peptide ring size was also investigated in the series *cyclo*[(-L-Phe-D-^{Me}*N*-Ala)$_n$-] ($n = 3-6$), and only parent peptide **1** ($n = 4$) displayed evidence of solution dimerization, presumably due to optimal structural rigidity of the cyclic D,L-octapeptide ring and attendant preorganization for self-assembly.

Finally, preliminary results suggest that, like natural protein and peptide secondary structures, the stability of cyclic D,L-octapeptide dimers is influenced by amino acid composition. Replacement of two phenylalanines in parent peptide **1** with Leu or Hag to give **9** and **10**, respectively, resulted in reduced association constants (Table 1), consistent with the high propensity of Phe for β-sheet conformations.[35a,39−42] In keeping with this interpretation, incorporation of flexible sarcosine (*N*-methylglycine) residues in peptide **13** completely abolished solution self-association. These findings indicate that dimer-forming cyclic D,L-peptides may prove useful as well-behaved model systems for evaluation of amino acid β-sheet propensities.[44]

Experimental Section

Chemicals. Acetonitrile (optima grade), dichloromethane (ACS grade), and dimethylformamide (sequencing grade) were purchased from Fisher and used without further purification. Diisopropylethylamine (*i*-Pr$_2$NEt, peptide synthesis grade) was purchased from Fisher and distilled first from ninhydrin and then from CaH_2 and stored over KOH pellets.[45a] Trifluoroacetic acid (TFA, New Jersey Halocarbon), 2-(1*H*-benzotriazol-1-yl)-1,1,3,3-tetramethyluronium hexafluorophosphate (HBTU, Richelieu Biotechnologies), *O*-(7-azabenzotriazol-1-yl)-1,1,3,3-tetramethyluronium hexafluorophosphate (HATU, PerSeptive Biosystems),[45b−d] 1-hydroxy-7-azabenzotriazole (HOAt, PerSeptive Biosystems), anisole (anhydrous, Aldrich), tetrabutylammonium fluoride hydrate ($Bu_4NF\cdot xH_2O$, 98%, Aldrich), tetrabutylammonium hydrogen sulfate (Bu_4NHSO_4, 99%, Fluka), and hydrogen fluoride (anhydrous, Matheson) were used without further purification. Commercially available *N*-Boc-amino acids were used as obtained from Bachem, Novabiochem, or Advanced Chemtech. Commercially available *N*-Boc-aminoacyl-4-(oxymethyl)phenylacetamidomethyl polystyrene resins (*N*-Boc-aminoacyl-OCH$_2$-Pam resins) were used as obtained from Applied Biosystems, Bachem, or Novabiochem, and aminomethylated polystyrene resin was used as obtained from Peptides International. $CDCl_3$ (99.8%, Isotech) for ^{1}H NMR spectroscopy was dried over 4-Å molecular sieves or distilled from P_2O_5 under Ar prior to use, while $CHCl_3$ (Optima, Fisher) for solution IR spectroscopy was used as obtained.

Synthesis of Amino Acids and Derivatives. Commercially unavailable *N*-Boc-aminoacyl-OCH$_2$-Pam resins were typically prepared using the preferred method of Kent and co-workers.[46] *N*-Boc-L-homoallylglycine (Hag) was synthesized from diethyl acetamidomalonate and 4-bromo-1-butene according to the procedure of Coulter and Talalay,[47a] resolved (porcine kidney acylase I) according to the procedure of Whitesides and co-workers,[47b] and Boc-protected using standard methods. *N*-Boc-*N*-alkylamino acids were prepared from the corresponding *N*-Boc-amino acids as described by Cheung and Benoiton.[48]

Peptide Synthesis and Cyclization. Unless otherwise noted, manual Boc solid-phase synthesis (SPPS) of linear peptides was carried out in a stepwise fashion according to the *in situ* neutralization protocol of Kent[49] and employing *N*-Boc-aminoacyl-OCH$_2$-Pam resins (∼0.4−0.8

(44) For other studies of amino acid β-sheet propensities in organic solvents, see: (a) Kemp, D. S.; Bowen, B. R.; Muendel, C. C. *J. Org. Chem.* **1990**, *55*, 4650−4657. (b) Nowick, J. S.; Insaf, S. *J. Am. Chem. Soc.* **1997**, *119*, 10903−10908.

(45) (a) Carpino, L. A.; El-Faham, A. *J. Org. Chem.* **1994**, *59*, 695−698. (b) Carpino, L. A. *J. Am. Chem. Soc.* **1993**, *115*, 4397−4398. (c) Carpino, L. A.; El-Faham, A.; Minor, C. A.; Albericio, F. *J. Chem. Soc., Chem. Commun.* **1994**, 201−203. (d) Ehlrich, A.; Rothemund, S.; Brudel, M.; Carpino, L. A.; Beinert, M. *Tetrahedron Lett.* **1993**, *34*, 4781−4784.

(46) Tam, J. P.; Kent, S. B.; Wong, T. W.; Merrifield, R. B. *Synthesis* **1979**, 955−957.

(47) (a) Coulter, A. W.; Talalay, P. *J. Biol. Chem.* **1968**, *243*, 3238−3247. (b) Chenault, H. K.; Dahmer, J.; Whitesides, G. M. *J. Am. Chem. Soc.* **1989**, *111*, 6354−6364.

(48) (a) Cheung, S. T.; Benoiton, N. L. *Can. J. Chem.* **1977**, *55*, 906−921. (b) In the case of *N*-Boc-L-^{All}*N*-Ala and *N*-Boc-L-^{Pen}*N*-Ala, allyl bromide and 5-bromo-1-butene, respectively, were used as electrophiles in the presence of catalytic NaI; in addition, DMF was used in place of THF as the reaction solvent.

(49) Schnolzer, M.; Alewood, P.; Jones, A.; Alewood, D.; Kent, S. B. H. *Int. J. Pept. Protein Res.* **1992,** *40*, 180−193.

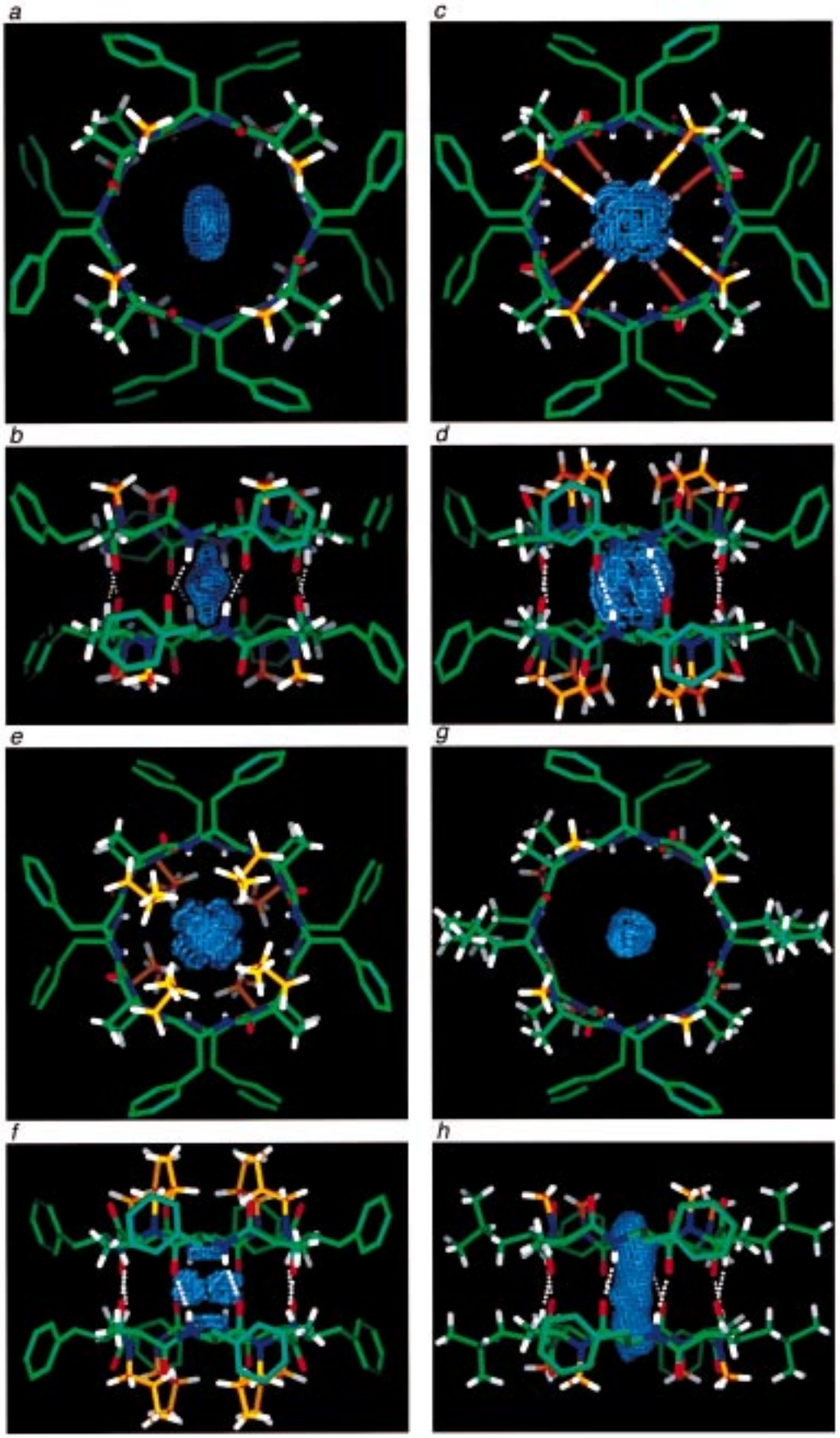

Figure 9. Crystal structures of dimeric β-sheet assemblies formed by (a) and (b) *cyclo*[(-L-Phe-D-^{Me}*N*-Ala)$_4$-] (**1**); (c) and (d) *cyclo*[(-D-Phe-L-^{All}*N*-Ala)$_4$-] (**2**); (e) and (f) *cyclo*[(-D-Phe-L-^{Pr}*N*-Ala)$_4$-] (**3**); and (g) and (h) *cyclo*[(-L-Phe-D-^{Me}*N*-Ala-L-Leu-D-^{Me}*N*-Ala)$_2$-] (**9**), as viewed down the cylindrical axis and across the dimeric interface, respectively. Electron density for encapsulated water is indicated in blue and represents time-averaged positions of overlapping water binding sites.

mequiv/g loading), as indicated for each peptide. Amino acid activation was typically accomplished using HBTU; however, HATU provided more complete aminoacylation of hindered secondary amino termini. Owing to higher acylation rates of OAt versus OBt esters,[45b−d] HATU activation was also employed during the second coupling step (third residue) in order to minimize diketopiperazine formation and attendant chain loss.

Peptides were cleaved from resin using standard HF procedures (10 mL of 9:1 (v/v) HF/anisole per gram of peptidyl resin; 1 h at 0 °C) or, for those peptides bearing acid-sensitive olefin functionalities, basic hydrolysis ($Bu_4NF{\cdot}xH_2O$/DMF[50a] or Bu_4NHSO_4/K_2CO_3/THF/H_2O[50b])[50c] and eluted with DMF. Following purification by reversed-phase high-performance liquid chromatography (RP-HPLC/C_4 column/CH_3CN/H_2O/0.1% TFA), cyclization was typically effected as indicated in the following representative procedure for peptide **12**:

An oven-dried 250-mL round-bottom flask equipped with a magnetic stir bar was charged with 1 equiv of linear peptide TFA·(-L-Phe-D-^{Me}*N*-Ala-L-VaL-D-^{Me}*N*-Ala)$_2$ (**12-x**) (98 mg, 102 μmol), 1.2 equiv of HATU (46 mg, 122 μmol), and 1.0 equiv of HOAt (14 mg, 102 μmol) and then purged with Ar. DMF was added via syringe (102 mL), and the flask was cooled to 0 °C in an ice bath under a positive pressure of Ar. *i*-Pr_2NEt was added dropwise (3 equiv, 53 μL, 306 μmol) with stirring, and the resulting reaction mixture was left for 2 h at 0 °C. After removal of solvent under reduced pressure, the crude cyclic peptide was dissolved in 10 mL of 2:1 (v/v) CH_3CN/H_2O and purified by RP-HPLC to afford 52 mg (62 μmol, 61%) of **12**.

***cyclo*[(-L-Phe^1-D-^{Me}*N*-Ala^2)$_4$-] (1).** Linear octapeptide (-L-Phe-D-^{Me}*N*-Ala)$_4$ (**1-x**) was synthesized on *N*-Boc-D-^{Me}*N*-Ala-(OCH$_2$)-Pam resin (0.73 mmol scale) and cleaved with HF to give 133 mg of the desired product as its TFA salt after purification by RP-HPLC (125 μmol, 17%; ESI-MS, $[M + H]^+$ calcd = 947.5, found = 947). A truncated side product, linear hexapeptide (-L-Phe-D-^{Me}*N*-Ala)$_3$ (**15-x**) (presumably caused by diketopiperazine chain termination in the second coupling step), was isolated in 9% purified yield (48 mg, 58 μmol). Cyclization of 38 mg of **1-x** (36 μmol) and purification as described above afforded 23 mg of **1** (24 μmol, 67%). ^{1}H NMR (500 MHz, 293 K, 2.0 mM, $CDCl_3$): **L-Phe^1**, N−H (**m** 6.98, d, J = 7.5 Hz; **d** 8.73, d, J = 8.5 Hz), C$^\alpha$H (**m** 4.85, m; **d** 5.27, m), C$^\beta$H$_2$ (**m**, **d** 2.92−3.03, m), C$^{\delta,\epsilon,\xi}$H (**m**, **d** 7.15−7.26, m); **D-^{Me}*N*-Ala^2**, N−CH_3 (**m** 2.49, s; **d** 2.77, s), C$^\alpha$H (**m** 5.21, q, J = 7.3 Hz; **d** 5.84, q, J = 6.9 Hz), C$^\beta$H$_3$ (**m** 1.14, d, J = 7.1 Hz; **d** 0.99, d, J = 6.8 Hz). IR (293 K, 1 mM, $CHCl_3$): 3309 (amide A); 1628, 1677 (amide I$_\perp$); 1523 (amide II$_{||}$). ESI-MS: $[M + H]^+$ calcd = 929.5, found = 929.

***cyclo*[(-D-Phe^1-L-^{All}*N*-Ala^2)$_4$-] (2).** Linear octapeptide (-D-Phe-L-^{All}*N*-Ala)$_4$ (**2-x**) was synthesized on *N*-Boc-L-^{All}*N*-Ala-(OCH$_2$)-Pam resin (1 mmol scale) and cleaved with $Bu_4NF{\cdot}xH_2O$[50c] (270 mg of crude; ESI-MS, $[M + H]^+$ calcd = 1051.6, found = 1051). Cyclization of 135 mg of the crude material and purification as described above afforded 12 mg of **2** (12 μmol, 2.4% overall). ^{1}H NMR (500 MHz, 293 K, 3.0 mM, $CDCl_3$): **D-Phe^1**, N−H (**m** 6.79, d, J = 7.0 Hz; **d** 8.71, d, J = 8.5 Hz), C$^\alpha$H (**m** 4.82, m; **d** 5.05, m), C$^\beta$H$_2$ (**m** 2.98, m; **d** 3.01, m), C$^{\delta,\epsilon,\xi}$H (**m**, **d** 7.16−7.27, m); **L-^{All}*N*-Ala^2**, N−C*H*$_2$CHCH$_2$ (**m** 3.49, 4.02, m; **d** 3.39, 4.19, m), N−CH$_2$C*H*CH$_2$ (**m** 5.45, m; **d** 5.59, m), N−CH$_2$CHC*H*$_2$ (**m** 4.85 (*E*), 4.99 (*Z*), m; **d** 4.91 (*E* and *Z*), m), C$^\alpha$H (**m** 5.32, q, J = 7.0 Hz; **d** 5.93, q, J = 6.5 Hz), C$^\beta$H$_3$ (**m** 1.24, d, J = 7.0 Hz; **d** 1.02, d, J = 6.5 Hz). ESI-MS: $[M + H]^+$ calcd = 1033.6, found = 1033.

***cyclo*[(-D-Phe^1-L-^{Pr}*N*-Ala^2)$_4$-] (3).** To a 5-mL round-bottom flask equipped with magnetic stir bar were added 2.5 mg of tetra-*N*-allyl cyclic octapeptide **2** (2.4 μmol) and 2.5 mg of 10% Pd−C (10% (w/w) catalyst). The flask was then purged with N_2 and charged with 1 mL of absolute EtOH. After sparging with H_2, the mixture was stirred 12 h under 1 atm H_2. Filtration through Celite and purification by RP-HPLC afforded 2 mg of tetra-*N*-(*n*-propyl) peptide **3** (1.9 μmol, 80%). ^{1}H NMR (400 MHz, 293 K, 2.0 mM, $CDCl_3$): **D-Phe^1**, NH (**m** 7.12, br; **d** 8.86, d, J = 8.7 Hz), C$^\alpha$H (**m** 4.93, m; **d** 5.23, m), C$^\beta$H$_2$ (**m** 2.93, 3.08, m; **d** 3.02, 3.12, m), C$^{\delta,\epsilon,\xi}$H (**m**, **d** 7.16−7.32, m); **L-^{Pr}*N*-Ala^2**, N−C*H*$_2$CH$_2$CH$_3$ (**m** 2.71, 3.16, m, **d** 2.67, 3.51, m), N−CH$_2$C*H*$_2$CH$_3$ (**m** 1.09, 1.25, m; **d** 1.26, 1.27, m), N−CH$_2$CH$_2$C*H*$_3$ (**m** 0.80, m; **d** 0.72, m), C$^\alpha$H (**m** 4.86, br; **d** 5.73, q, J = 6.4 Hz), C$^\beta$H$_3$ (**m** 1.25, ovl; **d** 0.89, d, J = 6.5 Hz). IR (293 K, 1 mM, $CHCl_3$): 3306 (amide A); 1625, 1675 (amide I$_\perp$); 1525 (amide II$_{||}$). ESI-MS: $[M + H]^+$ calcd = 1041.6, found = 1042.

cyclo*[(-D-Phe^1-L-^{All}*N*-Ala^2-D-Phe^3-L-Ala^4)$_2$-] (4).** Linear octapeptide (-D-Phe-L-^{All}*N*-Ala-D-Phe-L-Ala)$_2$ (**4-x**) was synthesized on *N*-Boc-D-Phe-(OCH$_2$)-Pam resin (0.5 mmol scale) and cleaved with $Bu_4NF{\cdot}xH_2O$ (350 mg of crude; ESI-MS, $[M + H]^+$ calcd = 971.5, found = 972). Cyclization of 300 mg of the crude material and purification as described above afforded 100 mg of **4** (105 μmol, 21% overall). ^{1}H NMR (400 MHz, 293 K, 20 mM, $CDCl_3$): **D-Phe^1**, N−H (**m** 7.55, d, J = 9.5 Hz; **d** 8.40, d, J = 11.5 Hz; **d 8.70, d, J = 11.6 Hz), C$^\alpha$H (**m** 4.78, m; **d** 4.55, m; **d*** 4.40, m), C$^\beta$H$_2$ (**m** 2.92, 3.23, m; **d** 2.90, 3.01, m; **d*** 2.76, 3.17, m), C$^{\delta,\epsilon,\xi}$H (**m**, **d**, **d*** 7.14−7.35, m); **L-^{All}*N*-Ala^2**, N−C*H*$_2$CHCH$_2$ (**m** 3.63, 4.52, m; **d** 3.95, 4.40, m; **d*** 4.30, 4.50, m), N−CH$_2$C*H*CH$_2$ (**m** 5.60, m; **d** 5.71, m; **d*** 5.84, m), N−CH$_2$CHC*H*$_2$ (**m** 4.87 (*E* and *Z*), m; **d** 5.07 (*E*), 5.42 (*Z*), m; **d*** 5.16 (*E* and *Z*), m), C$^\alpha$H (**m** 5.16, ovl; **d** 5.36, q, J = 8.8 Hz; **d*** 5.90, ovl), C$^\beta$H$_3$ (**m** 1.12, d, J = 8.8 Hz; **d** 1.16, d, J = 8.8 Hz; **d*** 1.23, d, J = 9.4 Hz); **d-Phe^3**, N−H (**m** 7.12, ovl; **d** 8.47, d, J = 10.2 Hz **d*** 8.36, d, J = 9.5 Hz), C$^\alpha$H (**m** 5.09, m; **d** 4.63, m; **d*** 5.08, m), C$^\beta$H$_2$ (**m** 2.81, 2.94, m; **d** 2.95, m; **d*** 2.85, 2.94, m), C$^{\delta,\epsilon,\xi}$H (**m**, **d**, **d*** 7.14−7.35, m); **L-Ala^4**, N−H (**m** 6.36, d, J = 7.5 Hz; **d** 6.30, d, J = 9.5 Hz; **d*** 6.19, d, J = 10.2 Hz), C$^\alpha$H (**m** 4.47, ovl; **d** 4.97, ovl; **d*** 4.70, ovl), C$^\beta$H$_3$ (**m** 1.19, d, J = 8.8 Hz; **d** 0.90, d, J = 8.2 Hz; **d*** 0.67, d, J = 8.2 Hz). ESI-MS: $[M + H]^+$ calcd = 953.5, found = 954.

cyclo*[(-D-Phe^1-L-^{Pr}*N*-Ala^2-D-Phe^3-L-Ala^4)$_2$-] (5).** To a 5-mL round-bottom flask equipped with a magnetic stir bar were added 6 mg of di-*N*-allyl cyclic octapeptide **4** (6.3 μmol) and 10 mg of 10% Pd−C (17% (w/w) catalyst). The flask was then purged with N_2 and charged with 1 mL of absolute EtOH. After sparging with H_2, the mixture was stirred 24 h under 1 atm H_2. Filtration through Celite afforded di-*N*-(*n*-propyl) peptide **5** in essentially quantitative yield. ^{1}H NMR (400 MHz, 293 K, 2.0 mM, $CDCl_3$; resonances labeled **x**−**z** could not be assigned unambiguously to **m**, **d**, or **d): **D-Phe^1**, N−H (**m** 7.44, d, J = 7.6 Hz; **d** 8.54, d, J = 9.7 Hz; **d*** 8.88, d, J = 9.7 Hz), C$^\alpha$H (**m** 4.87, m; **d*** 5.18, m; **d** 5.16, m), C$^\beta$H$_2$ (**m** 2.95, 3.23, m; **d** 2.85, 2.97, m; **d*** 2.85, 2.97, m), C$^{\delta,\epsilon,\xi}$H (**m**, **d**, **d*** 7.15−7.32, m); **L-^{Pr}*N*-Ala^2**, N−C*H*$_2$CH$_2$CH$_3$ (**x** 2.95, 3.60, m; **y** 2.95, 3.60, m; **z** 2.88, m), NCH$_2$C*H*$_2$CH$_3$ (**x** 1.63, 1.85, m; **y** 1.45, 1.58, m; **z** 1.10, m), N−CH$_2$-CH$_2$C*H*$_3$ (**x** 0.92, m; **y** 0.86, m; **z** 0.67, m), C$^\alpha$H (**m** 5.12, ovl; **d** 5.29, q, J = 6.5 Hz; **d*** 5.77, q, J = 6.0 Hz), C$^\beta$H$_3$ (**m** 1.17, ovl; **d** 1.07, d, J = 6.5 Hz; **d*** 1.11, ovl); **D-Phe^3**, N−H (**m** 7.24, ovl; **d** 8.50, d, J = 8.1 Hz; **d*** 8.38, d, J = 7.6 Hz), C$^\alpha$H (**m** 4.61, m; **d** 4.57, m; **d*** 4.37, m), C$^\beta$H$_2$ (**m** 2.93, 3.06, m; **d** 2.88, 3.06, m; **d*** 2.78, 3.26, m), C$^{\delta,\epsilon,\xi}$H (**m**, **d***, **d** 7.15−7.32, m); **L-Ala^4**, N−H (**m** 6.33, d, J = 5.9 Hz; **d** 6.30, d, J = 8.1 Hz; **d*** 6.26, ovl), C$^\alpha$H (**m** 4.46, ovl; **d** 5.02, ovl; **d*** 4.81, ovl), C$^\beta$H$_3$ (**m** 1.18, ovl; **d** 0.87, d, J = 6.5 Hz; **d*** 0.71, d, J = 7.0 Hz). IR (293 K, 1 mM, $CHCl_3$): 3306 (amide A); 1628, 1655, 1688 (amide I$_\perp$); 1515 (amide II$_{||}$). ESI-MS: $[M + H]^+$ calcd = 957.5, found = 957.

***bicyclo*[(-D-Phe^1-L-*N*-(dithiopropyl)-Ala^2-D-Phe^3-L-Ala^4)$_2$-] (6).** Dipeptide *N*-Boc-D-Phe-L-*N*-(3-(4-MeBn)thiopropyl)-Ala (**6-w**) was prepared as follows: An oven-dried 500-mL round-bottom flask was purged with Ar and charged with 4 g of *N*-Boc-D-Phe-L-^{All}*N*-Ala-OBn (**6-u**) (8.6 mmol, 1equiv, prepared via standard solution-phase peptide synthesis), 160 mL of dry toluene (freshly distilled under argon), and 3.47 mL of 4-methylbenzylmercaptan. While excluding light and purging with Ar, 1.2 g of freshly recrystallized AIBN was added. The reaction mixture was kept under Ar and heated at 80 °C for 24 h in the dark. The solvent was then removed under reduced pressure, and the resulting residue was purified via SiO_2 flash chromatography (10→40% EtOAc/hexanes) to give 4.2 g of *N*-Boc-D-Phe-L-*N*-(3-(4-MeBn)-thiopropyl)-Ala-OBn (**6-v**) (7 mmol, 81%). LiOH hydrolysis and SiO_2 flash chromatography (7.5% MeOH in CH_2Cl_2) afforded the desired

(50) (a) Ueki, M.; Kai, K.; Amemiya, M.; Horino, H.; Oyamada, H. *J. Chem. Soc. Chem. Commun.* **1988**, 414−415. (b) Spatola, A. F.; Anwer, M. K.; Rao, M. N. *Int. J. Pept. Protein Res.* **1992**, *40*, 322−332. (c) Our experience indicates that basic cleavage of peptidyl-OCH$_2$-Pam resins with either $Bu_4NF{\cdot}xH_2O$/DMF[50a] or Bu_4NHSO_4/K_2CO_3/THF/H_2O[50b] can lead to considerable C-terminal epimerization in cases where the C-terminal residue bears a tertiary backbone amide function.

dipeptide **6-w** as its free acid in 51% yield (ESI-MS, $[M - H]^-$ calcd = 512.3, found = 513).

Peptide *cyclo*[(-D-Phe-L-*N*-(3-(4-MeBn)thiopropyl)-Ala-D-Phe-L-Ala)$_2$-] (**6-y**) was prepared as follows: Linear octapeptide (-L-Ala-D-Phe-L-*N*-(3-(4-MeBn)thiopropyl)-Ala-D-Phe)$_2$ (**6-x**) was synthesized on *N*-Boc-D-Phe-(OCH$_2$)-Pam resin (0.56 mmol scale) using *N*-Boc-protected D-Phe and L-Ala as well as protected dipeptide *N*-Boc-D-Phe-L-*N*-(3-(4-MeBn)thiopropyl)-Ala (**6-w**) and cleaved with $Bu_4NF\cdot xH_2O$ (300 mg of crude; ESI-MS, $[M + H]^+$ calcd = 1246, found = 1248). Cyclization of 300 mg of the crude material as described above afforded 150 mg of **6-y** (122 μmol, 22%) after purification by RP-HPLC. ESI-MS: $[M + H]^+$ calcd = 1228, found = 1230.

To a 10-mL round-bottom flask equipped with a magnetic stir bar was added 110 mg of *cyclo*[(-D-Phe-L-*N*-(3-(4-MeBn)thiopropyl)-Ala-D-Phe-L-Ala)$_2$-] (**6-y**) (90 μmol, 1 equiv) followed by 5 mL of TFA and 19.5 μL of anisole. The solution was cooled to 4 °C, treated with 53.5 mg of Tl(CF$_3$CO$_2$)$_3$, and stirred at 4 °C for 18 h. After evaporation of the solvent under a stream of nitrogen, the resulting residue was subjected to purification by RP-HPLC to give 20 mg of the desired bicyclic product **6** (20 μMol, 22%). ^{1}H NMR (500 MHz, 293 K, 10.0 mM, CDCl$_3$): **D-Phe^1**, N−H (**m** 7.20, br; **d** 8.19, br), C$^\alpha$H (**m** 4.91, m; **d** 5.38, m), C$^\beta$H$_2$ (**m** 3.07, m; **d** 2.76, 2.95, m), C$^{\delta,\epsilon,\xi}$H (**m**, **d** 7.05−7.31, m); **L-*N*-(dithiopropyl)-Ala^2**, N−C*H*$_2$CH$_2$CH$_2$S− (**m** 2.83, 3.19, m; **d** 3.17, 3.59, m), N−CH$_2$C*H*$_2$CH$_2$S− (**m** 1.43, 1.56, m; **d** 1.57, 1.69, m), N−CH$_2$CH$_2$C*H*$_2$S− (**m** 1.94, 2.11, m; **d** 2.50, 3.29, m), C$^\alpha$H (**m** 5.15, br; **d** 4.73, br); C$^\beta$H$_3$ (**m** 1.11, br s; **d** 0.83, br s); **D-Phe^3**, N−H (**m** 7.73, br; **d** 8.01, br), C$^\alpha$H (**m** 4.61, m; **d** 4.68, m), C$^\beta$H$_2$ (**m** 2.85, 2.99, m; **d** 3.00, m), C$^{\delta,\epsilon,\xi}$H (**m**, **d** 7.05−7.31, m); **L-Ala^4**, N−H (**m** 6.30, br; **d** 6.81, br), C$^\alpha$H (**m** 4.51, br; **d** 5.00, br), C$^\beta$H$_3$ (**m** 1.12, br s; **d** 1.08, br s). ESI-MS: $[M + H]^+$ calcd = 1019.5, found = 1020.

cyclo*[(-D-Phe^1-L-^{Pen}*N*-Ala^2-D-Phe^3-L-Hag^4)$_2$-] (7).** Linear octapeptide (-D-Phe-L-^{Pen}*N*-Ala-D-Phe-L-Hag)$_2$ (**7-x**) was synthesized on *N*-Boc-L-Hag-(OCH$_2$)-Pam resin (0.4 mmol scale) and cleaved with $Bu_4NF\cdot xH_2O$ to give 143 mg of the desired product as its TFA salt after purification by RP-HPLC (117 μmol, 29%). Cyclization of 143 mg of **7-x** (117 μmol) and purification as described above afforded 67 mg of **7** (62 μmol, 53%). ^{1}H NMR (500 MHz, 293 K, CDCl$_3$): **D-Phe^1**, N−H (**m** 7.56, br; **d 8.69, d, J = 9.5 Hz; **d** 9.04, d, J = 9.5 Hz), C$^\alpha$H (**m** 4.87, m; **d*** 5.34, m; **d** 5.33, m), C$^\beta$H$_2$ (**m** 3.00, 3.25, m; **d** 2.87, 2.99, m; **d *** 2.85, 3.27, m), C$^{\delta,\epsilon,\xi}$H (**m**, **d**, **d*** 7.02−7.46, m); **L-^{Pen}*N*-Ala^2**, N−C*H*$_2$CH$_2$CH$_2$CHCH$_2$ (**m** 2.93, 2.94, m; **d** 3.02, 3.57, m; **d*** 3.06, 3.66, m), N−CH$_2$C*H*$_2$CH$_2$CHCH$_2$ (**m** 1.07, 1.19, m; **d** 1.70, 1.77, m; **d***1.86, 1.95, m), N−CH$_2$CH$_2$C*H*$_2$CHCH$_2$ (**m** 1.84, m; **d** 2.02, 2.17, m; **d*** 2.08, 2.24, m), N−CH$_2$CH$_2$CH$_2$C*H*CH$_2$ (**m** 5.61, m; **d** 5.90, m; **d*** 5.95, m), N−CH$_2$CH$_2$CH$_2$CHC*H*$_2$ (**m** 4.89 (*E*), 4.93 (*Z*), m; **d** 5.08 (*E* and *Z*), m; **d*** 5.09 (*Z*), 5.13 (*E*), m), C$^\alpha$H (**m** 5.12, ovl; **d** 5.79, ovl; **d*** 5.48, ovl), C$^\beta$H$_3$ (**m** 1.16, ovl; **d** 1.13, d, J = 6.8 Hz; **d*** 1.06, d, J = 7.4 Hz); **D-Phe^3**, N−H (**m** 7.30, br; **d** 8.50, d, J = 7.5 Hz; **d*** 8.69, d, J = 8.1 Hz), C$^\alpha$H (**m** 4.73, m; **d** 4.53, m; **d*** 4.63, m), C$^\beta$H$_2$ (**m** 2.97, 3.02, m; **d** 2.77, 3.27, m; **d*** 2.88, 3.09, m), C$^{\delta,\epsilon,\xi}$H (**m**, **d**, **d*** 7.02−7.46, m); **L-Hag^4**, N−H (**m** 6.56, d, J = 8.1 Hz; **d** 6.51, d, J = 8.2 Hz; **d*** 6.45, br), C$^\alpha$H (**m** 4.61, m; **d** 4.94, m; **d*** 5.16, m), C$^\beta$H$_2$ (**m** 1.69, 1.78, m; **d** 1.06, 1.20, m; **d*** 1.20, 1.28, m), C$^\gamma$H$_2$ (**m** 1.89, m; **d** 1.14, m; **d*** 1.52, m), C$^\delta$H (**m** 5.75, m; **d** 5.45, m; **d*** 5.55, m), C$^\epsilon$H$_2$ (**m** 5.01 (*E* and *Z*), m; **d** 4.77 (*E*), 4.90 (*Z*), m; **d*** 4.83 (*E*), 4.93 (*Z*), m). IR (293 K, 1 mM, CHCl$_3$): 3304 (amide A); 1627, 1654, 1687 (amide I$_\perp$); 1523 (amide II$_\parallel$). ESI-MS: $[M + H]^+$ calcd = 1089.6, found = 1090.

cyclo*[(-D-Phe^1-L-^{Pen}*N*-Ala^2-D-Phe^3-L-^{Me}*N*-Hag^4)$_2$-] (8).** Linear octapeptide (-D-Phe-L-^{Pen}*N*-Ala-D-Phe-L-^{Me}*N*-Hag)$_2$ (**8-x**) was synthesized on *N*-Boc-L-^{Me}*N*-Hag-(OCH$_2$)-Pam resin (0.4 mmol scale) and cleaved with $Bu_4NHSO_4-K_2CO_3$[50c] to give 281 mg of the desired product as its TFA salt after purification by RP-HPLC (225 μmol, 56%). Cyclization of 281 mg of **8-x** (225 μmol) and purification as described above afforded 35 mg of **8** (35 μmol, 16%). ^{1}H NMR (500 MHz, 293 K, CDCl$_3$): **D-Phe^1**, N−H (**m$_1$** 8.50, d, J = 6.8 Hz; **m$_2$** 7.00, d, J = 10.2 Hz; **d** 8.87, d, J = 8.9 Hz; **d 8.77, d, J = 9.5 Hz), C$^\alpha$H (**m$_1$** 4.63, m; **m$_2$** 4.91, m; **d** 5.41, m; **d*** 5.49, m), C$^\beta$H$_2$ (**m$_1$** 2.56, 2.69, m; **m$_2$** 2.99, 3.12, m; **d** 3.05, 3.10, m; **d*** 3.03, 3.06, m), C$^{\delta,\epsilon,\xi}$H (**m$_1$**, **m$_2$**, **d**, **d*** 7.03−7.46, m); **L-^{Pen}*N*-Ala^2**, N−C*H*$_2$CH$_2$CH$_2$CHCH$_2$ (**m$_1$** 3.31, 3.49, m; **m$_2$** 2.71, 3.34, m; **d** 2.97, 3.47, m; **d*** 2.87, 3.56, m), N−CH$_2$C*H*$_2$-CH$_2$CHCH$_2$ (**m$_1$** 1.77, 1.92, m; **m$_2$** 1.10, 1.29, m; **d** 1.61, 1.62, m; **d*** 1.64, 1.77, m), N−CH$_2$CH$_2$C*H*$_2$CHCH$_2$ (**m$_1$** 2.02, 2.21, m; **m$_2$** 1.93, m; **d** 2.01, 2.08, m; **d*** 1.88, 2.13, m), N−CH$_2$CH$_2$CH$_2$C*H*CH$_2$ (**m$_1$**, **m$_2$**, **d**, **d*** 4.92−5.87, m), C$^\alpha$H (**m$_1$** 5.08, ovl; **m$_2$** 3.63, ovl; **d** 5.77, ovl; **d*** 5.87, ovl), C$^\beta$H$_3$ (**m$_1$** 1.36, ovl, d, J = 7.4 Hz; **m$_2$** 1.58, d, J = 6.8 Hz; **d** 0.95, d, J = 6.8 Hz; **d*** 1.05, d, J = 6.8 Hz); **D-Phe^3**, N−H (**m$_1$** 7.92, d, J = 6.1 Hz; **m$_2$** 6.95, d, J = 6.8 Hz; **d** 8.74, d, J = 8.8 Hz; **d*** 8.93, *d*, J = 9.4 Hz), C$^\alpha$H (**m$_1$** 5.02, m; **m$_2$** 5.06, m; **d** 5.48, m; **d*** 5.44, m), C$^\beta$H$_2$ (**m$_1$** 2.98, 3.01, m; **m$_2$** 2.97, 3.01, m; **d** 3.03, 3.06, m; **d*** 3.05, 3.10), C$^{\delta,\epsilon,\xi}$H (**m$_1$**, **m$_2$**, **d**, **d*** 7.03−7.46, m); **L-^{Me}*N*-Hag^4**, N−CH$_3$ (**m$_1$** 2.99, s; **m$_2$** 2.67, s; **d** 2.98, s; **d*** 2.85, s), C$^\alpha$H (**m$_1$** 5.10, m; **m$_2$** 4.54, m; **d** 5.68, m; **d*** 5.62, m), C$^\beta$H$_2$ (**m$_1$** 1.58, 1.91, m; **m$_2$** 1.49, 1.77, m; **d** 1.30, 1.62, m; **d*** 1.12, 1.66, m), C$^\gamma$H$_2$ (**m$_1$**, **m$_2$** 1.49−2.21, m; **d** 1.81, m; **d*** 1.75, m), C$^\delta$H and C$^\epsilon$H$_2$ (**m$_1$**, **m$_2$**, **d**, **d*** 4.92−5.87, m). ESI-MS: $[M + H]^+$ calcd = 1117.6, found = 1118.

cyclo*[(-L-Phe^1-D-^{Me}*N*-Ala^2-L-Leu^3-D-^{Me}*N*-Ala^4)$_2$-] (9).** Linear octapeptide (-L-Leu-D-^{Me}*N*-Ala-L-Phe-D-^{Me}*N*-Ala)$_2$ (**9-x**) was synthesized on *N*-Boc-D-^{Me}*N*-Ala-(OCH$_2$)-Pam resin, cleaved with HF, and isolated as its TFA salt after purification by RP-HPLC (ESI-MS, $[M + H]^+$ calcd = 879.5, found = 880). Cyclization of 45 mg of **9-x** (46 μmol) and purification as described above afforded 26 mg of **9** (30 μmol, 65%). ^{1}H NMR (500 MHz, 293 K, 3.0 mM, CDCl$_3$): **L-Phe^1**, N−H (**m** 7.20, ovl; **d** 8.65, d, J = 8.2 Hz; **d 8.83, d, J = 8.2 Hz), C$^\alpha$H (**m** 4.83, m; **d** 5.26, m; **d*** 5.27, m), C$^\beta$H$_2$ (**m** 3.03, 3.14, m; **d** 2.81, 2.96, m; **d*** 2.91, 3.05, m), C$^{\delta,\epsilon,\xi}$H (**m**, **d**, **d*** 7.16−7.27, m); **D-^{Me}*N*-Ala^2**, N−CH$_3$ (**m** 2.62, s; **d** 2.79, s; **d*** 2.80, s), C$^\alpha$H (**m** 5.25, ovl; **d** 5.92, q, J = 6.8 Hz; **d*** 5.86), C$^\beta$H$_3$ (**m** 1.19, ovl; **d** 1.11, d, J = 6.8 Hz; **d*** 1.03, d, J = 6.8 Hz); **L-Leu^3**, N−H (**m** 6.92, d, J = 8.2 Hz; **d** 8.80, d, J = 9.5 Hz; **d*** 8.48, d, J = 8.8 Hz), C$^\alpha$H (**m** 4.60, m; **d** 5.14,; **d*** 5.09, m), C$^\beta$H$_2$ (**m** 1.37, 1.47, m; **d** 1.32, 1.56, m; **d*** 1.29, 1.43, m), C$^\gamma$H (**m** 1.66, m; **d** 1.61, m; **d*** 1.51, m), C$^{\delta1,\delta2}$H$_3$ (**m** 0.91, 0.92, ovl; **d** 0.82, d, J = 6.1 Hz, 0.95, ovl; **d*** 0.87, 0.93, ovl), **D-^{Me}*N*-Ala^4**, N−CH$_3$ (**m** 2.71, s; **d** 3.25, s; **d*** 3.27, s), C$^\alpha$H (**m** 5.26, ovl; **d** 5.79, q, J = 6.8 Hz; **d*** 5.86, ovl), C$^\beta$H$_3$ (**m** 1.26, ovl; **d** 1.15, d, J = 6.8 Hz; **d*** 1.23, ovl). ESI-MS: $[M + H]^+$ calcd = 861.5, found = 862.

cyclo*[(-L-Phe^1-D-^{Me}*N*-Ala^2-L-Hag^3-D-^{Me}*N*-Ala^4)$_2$-] (10).** Linear octapeptide (-D-^{Me}*N*-Ala-L-Hag-D-^{Me}*N*-Ala-L-Phe)$_2$ (**10-x**) was synthesized on *N*-Boc-L-Phe-(OCH$_2$)-Pam resin (0.54 mmol scale) and cleaved with $Bu_4NF\cdot xH_2O$ to give 230 mg of the desired product as its TFA salt after purification by RP-HPLC (233 μmol, 43%; ESI-MS, $[M + H]^+$ calcd = 875.5, found = 875). Cyclization of 112 mg of **10-x** (113 μmol) and purification as described above afforded 68 mg of **10** (79 μMol, 70%). ^{1}H NMR (500 MHz, 278 K, 7.5 mM, CDCl$_3$): **L-Phe^1**, N−H (**m** 7.21, ovl; **d** 8.60, d, J = 8.2 Hz; **d 8.82, d, J = 8.2 Hz), C$^\alpha$H (**m** 4.84, m; **d** 5.22, m; **d*** 5.25, m), C$^\beta$H$_2$ (**m** 2.98, 3.07, m; **d** 2.77, 2.95, m; **d*** 2.90, 3.02, m), C$^{\delta,\epsilon,\xi}$H (**m**, **d**, **d*** 7.18−7.30, m); **D-^{Me}*N*-Ala^2**, N−CH$_3$ (**m** 2.63, s; **d** 2.76, s; **d*** 2.74, s), C$^\alpha$H (**m** 5.27, ovl; **d** 5.96, ovl; **d*** 5.82, ovl), C$^\beta$H$_3$ (**m** 1.17, ovl; **d** 1.11, ovl; **d*** 1.01, d, J = 6.1 Hz); **L-Hag^3**, N−H (**m** 7.04, br; **d** 8.82, d, J = 8.2 Hz; **d*** 8.48, d, J = 8.1 Hz), C$^\alpha$H (**m** 4.54, m; **d** 5.07, m; **d*** 5.03, m), C$^\beta$H$_2$ (**m** 1.60, 1.73, m; **d** 1.59, 1.71, m; **d*** 1.50, 1.62, m), C$^\gamma$H$_2$ (**m** 2.01, m; **d** 2.07, m; **d*** 1.98, m), C$^\delta$H (**m** 5.65, m; **d** 5.74, m; **d*** 5.71, m), C$^\epsilon$H$_2$ (**m** 4.85 (*E*), 4.90 (*Z*), m; **d** 5.00 (*E*), 5.04 (*Z*), m; **d*** 4.89 (*E*), 4.94 (*Z*), m); **D-^{Me}*N*-Ala^4**, N−CH$_3$ (**m** 2.69, s; **d** 3.19, s; **d*** 3.22, s), C$^\alpha$H (**m** 5.20, ovl; **d** 5.76, ovl; **d*** 5.93, ovl), C$^\beta$H$_3$ (**m** 1.23, ovl; **d** 1.12, ovl; **d*** 1.20, ovl). IR (293 K, 1 mM, CHCl$_3$): 3310 (amide A); 1631, 1675 (amide I$_\perp$); 1527 (amide II$_\parallel$). ESI-MS: $[M + H]^+$ calcd = 857.5, found = 858.

cyclo*[(-L-Phe^1-D-^{Me}*N*-Ala^2-L-Ile^3-D-^{Me}*N*-Ala^4)$_2$-] (11).** Linear octapeptide (-L-Phe-D-^{Me}*N*-Ala-L-Ile-D-^{Me}*N*-Ala)$_2$ (**11-x**) was synthesized on *N*-Boc-D-^{Me}*N*-Ala-(OCH$_2$)-Pam resin (0.4 mmol scale) and cleaved with HF to give 100 mg of the desired product as its TFA salt after purification by RP-HPLC (101 μmol, 25%; ESI-MS, $[M + H]^+$ calcd = 879.5, found = 880). Cyclization of 100 mg of **11-x** (101 μmol) and purification as described above afforded 50 mg of **11** (58 μmol, 57%). ^{1}H NMR (500 MHz, 293 K, 22.1 mM, CDCl$_3$): **L-Phe^1**, N−H (**m** 7.05, br; **d** 8.71, d, J = 7.0 Hz; **d 8.87, d, J = 6.5 Hz), C$^\alpha$H (**m** 4.85, m; **d** 5.28, m; **d*** 5.28, m), C$^\beta$H$_2$ (**m** 3.04, m; **d** 2.93, 3.13, m; **d*** 2.91, 3.17, m), C$^{\delta,\epsilon,\xi}$H (**m**, **d**, **d*** 7.16−7.26, m); **D-^{Me}*N*-Ala^2**, N−CH$_3$ (**m** 2.55, s; **d** 2.81, s; **d*** 2.72, s), C$^\alpha$H (**m** 5.17, ovl; **d** 5.80, q, J = 6.8

Hz; **d*** 6.07, q, J = 5.5 Hz), $C^{\beta}H_3$ (**m** 1.18, d, J = 5.4 Hz; **d** 1.18, ovl; **d*** 1.11, d, J = 5.4 Hz); **L-Ile³**, N−H (**m** 6.94, br; **d** 8.63, d, J = 8.0 Hz; **d*** 8.44, d, J = 7.6 Hz), $C^{\alpha}H$ (**m** 4.55, m; **d** 4.92, m; **d*** 4.83, m), $C^{\beta}H$ (**m** 1.74, m; **d** 1.90,; **d*** 1.75, m), $C^{\gamma 1}H_2$ (**m** 1.11, 1.48, m; **d** 1.17, 1.55, m; **d*** 1.08, 1.46, m), $C^{\gamma 2}H_3$ (**m** 0.85, ovl; **d** 0.87, ovl; **d*** 0.83, ovl), $C^{\delta 1}H_3$ (**m** 0.87, ovl; **d** 0.80, ovl; **d*** 0.80, ovl); **D-^{Me}N-Ala⁴**, N−CH_3 (**m** 2.80, s; **d** 3.31, s; **d*** 3.30, s), $C^{\alpha}H$ (**m** 5.31, ovl; **d** 5.97, q, J = 6.8 Hz; **d*** 5.74, q, J = 5.4 Hz), $C^{\beta}H_3$ (**m** 1.32, d, J = 5.9 Hz; **d** 1.12, ovl; **d*** 1.26, d, J = 5.4 Hz). ESI-MS: $[M + H]^+$ calcd = 861.5, found = 861.5.

cyclo*[(-L-Phe¹-D-^{Me}N-Ala²-L-Val³-D-^{Me}N-Ala⁴)₂-] (12).** Linear octapeptide (-L-Phe-D-^{Me}N-Ala-L-VaL-D-^{Me}N-Ala)$_2$ (**12-x**) was synthesized on *N*-Boc-D-^{Me}N-Ala-(OCH$_2$)-Pam resin (0.4 mmol scale) and cleaved with HF to give 159 mg of the desired product as its TFA salt after purification by RP-HPLC (165 μmol, 41%; ESI-MS, $[M + H]^+$ calcd = 851.5, found = 851). Cyclization of 98 mg of **12-x** (102 μmol) and purification as described above afforded 52 mg of **12** (62 μmol, 61%). ^{1}H NMR (500 MHz, 293 K, 38.1 mM, $CDCl_3$): **L-Phe¹**, N−H (**m** 7.28, ovl; **d** 8.58, d, J = 8.8 Hz; **d 8.89, d, J = 8.1 Hz), $C^{\alpha}H$ (**m** 4.84, m; **d** 5.26; **d*** 5.24, m), $C^{\beta}H_2$ (**m** 3.03, m; **d** 2.82, 2.93, m; **d*** 2.90, 3.14, m), $C^{\delta,\epsilon,\xi}H$ (**m**, **d**, **d*** 7.16−7.27, m); **D-^{Me}N-Ala²**, N−CH_3 (**m** 2.61, s; **d** 2.80, s; **d*** 2.69, s), $C^{\alpha}H$ (**m** 5.07, ovl; **d** 5.85, br; **d*** 6.08, q, J = 7.4 Hz), $C^{\beta}H_3$ (**m** 1.18, d, J = 6.8 Hz; **d** 1.18, ovl; **d*** 1.10, d, J = 6.8 Hz); **L-Val³**, N−H (**m** 7.06, br; **d** 8.60, d, J = 8.8 Hz; **d*** 8.32, d, J = 9.5 Hz), $C^{\alpha}H$ (**m** 4.51, m; **d** 4.89, m; **d*** 4.83, m), $C^{\beta}H$ (**m** 1.96, m; **d** 2.03, m; **d*** 1.91, m), $C^{\gamma 1,\gamma 2}H_3$ (**m** 0.88, ovl; **d** 0.92, ovl; **d*** 0.86, ovl); **D-^{Me}N-Ala⁴**, N−CH_3 (**m** 2.84, s; **d** 3.02, s; **d*** 3.27, s), $C^{\alpha}H$ (**m** 5.18, ovl; **d** 5.93, br; **d*** 5.74, q, J = 6.7 Hz), $C^{\beta}H_3$ (**m** 1.26, d, J = 6.8 Hz; **d** 1.09, ovl; **d*** 1.23, ovl). IR (293 K, 1 mM, $CHCl_3$): 3317 (amide A); 1639, 1677 (amide $I_{\perp}$); 1524 (amide $II_{||}$). ESI-MS: $[M + H]^+$ calcd = 833.5; found = 834.

***cyclo*[(-L-Phe¹-Sar²)₄-] (13).** Linear octapeptide (-L-Phe-Sar)$_4$ (**13-x**) was synthesized on *N*-Boc-Sar-(OCH$_2$)-Pam resin (0.75 mmol scale) and cleaved with HF to give 358 mg of the desired product as its TFA salt after purification by RP-HPLC (356 μmol, 47%; ESI-MS, $[M + H]^+$ calcd = 891.4, found = 892). Cyclization of 60 mg of **13-x** (60 μmol) and purification as described above afforded 39 mg of **13** (45 μmol, 67%). ^{1}H NMR (500 MHz, 313 K, $CDCl_3$, major conformer only): **L-Phe¹**, N−H (6.90, d, J = 7.5 Hz), $C^{\alpha}H$ (5.06, m), $C^{\beta}H_2$ (2.94, 3.02, m), $C^{\delta,\epsilon,\xi}H$ (7.15−7.39, m); **Sar²**, N−CH_3 (2.78, s), $C^{\alpha}H_2$ (3.36, d, J = 15.1 Hz; 4.44, d, J = 15.1 Hz). ESI-MS: $[M + H]^+$ calcd = 873.4, found = 873.

***cyclo*[(-D-Phe¹-L-^{All}N-Ala²)₂-] (14).** Linear tetrapeptide (-D-Phe-L-^{All}N-Ala)$_2$ (**14-x**) was synthesized on *N*-Boc-L-^{All}N-Ala-(OCH$_2$)-Pam resin and cleaved with $Bu_4NF{\cdot}xH_2O$.[50c] Cyclization of 10 mg of the crude material (~19 μmol) and purification as described above afforded 2.2 mg of **14** (4.3 μmol, 22%). ^{1}H NMR (250 MHz, 293 K, $CDCl_3$): **D-Phe¹**, N−H (6.82, d, J = 10.4 Hz), $C^{\alpha}H$ (4.92, m), $C^{\beta}H_2$ (3.02, m), $C^{\delta,\epsilon,\xi}H$ (7.12−7.28, m); **L-^{All}N-Ala²**, N−CH_2CHCH_2 (3.69, 4.19, m), N−CH_2CHCH_2 (5.62, m), N−CH_2CHCH_2 (4.59 (*E*); 4.92 (*Z*), m), $C^{\alpha}H$ (5.18, q, J = 7.0 Hz), $C^{\beta}H_3$ (1.11, d, J = 7.1 Hz). ESI-MS: $[M - H]^-$ calcd = 515.3, found = 515.

***cyclo*[(-L-Phe¹-D-^{Me}N-Ala²)₃-] (15).** Linear hexapeptide (-L-Phe-D-^{Me}N-Ala)$_3$ (**15-x**) was isolated as its TFA salt in 9.3% yield (48 mg, 58 μmol; ESI-MS, MH^+ calcd = 715.4, found = 715) from the synthesis of linear octapeptide **1x** (*vide supra*). Cyclization of 24 mg of **15-x** (29 μmol) and purification as described above afforded 5.6 mg of **15** (8 μmol, 14%). ^{1}H NMR (500 MHz, 293 K, $CDCl_3$): **L-Phe¹**, N−H (7.54, d, J = 5.4 Hz), $C^{\alpha}H$ (4.92, m), $C^{\beta}H_2$ (2.83, 3.04, m), $C^{\delta,\epsilon,\xi}H$ (7.13−7.27, m); **D-^{Me}N-Ala²**, N−CH_3 (2.42, s), $C^{\alpha}H$ (4.86, br), $C^{\beta}H_3$ (1.07, d, J = 7.1 Hz). ESI-MS: $[M + H]^+$ calcd = 697.4, found = 697.

***cyclo*[(-L-Phe¹-D-^{Me}N-Ala²)₅-] (16).** Linear decapeptide (-L-Phe-D-^{Me}N-Ala)$_5$ (**16-x**) was synthesized on *N*-Boc-D-^{Me}N-Ala-(OCH$_2$)-Pam resin and cleaved with HF to give the desired product as its TFA salt after purification by RP-HPLC (ESI-MS, $[M + H]^+$ calcd = 1179.6, found = 1180). Cyclization of 47 mg of **16-x** (36 μmol) and purification as described above afforded 28 mg of **16** (24 μmol, 67%). ^{1}H NMR (400 MHz, 293 K, $CDCl_3$): **L-Phe¹**, N−H (7.15, ovl), $C^{\alpha}H$ (4.89, m), $C^{\beta}H_2$ (2.98, m), $C^{\delta,\epsilon,\xi}H$ (7.01−7.34, m); **D-^{Me}N-Ala²**, N−CH_3 (2.60, s), $C^{\alpha}H$ (4.98, br), $C^{\beta}H_3$ (1.11, br s). ESI-MS: $[M + H]^+$ calcd = 1161.6, found = 1161.

***cyclo*[(-L-Phe¹-D-^{Me}N-Ala²)₆-] (17).** Linear dodecapeptide (-L-Phe-D-^{Me}N-Ala)$_6$ (**17-x**) was synthesized on *N*-Boc-D-^{Me}N-Ala-(OCH$_2$)-Pam resin and cleaved with HF to give the desired product as its TFA salt after purification by RP-HPLC (ESI-MS, $[M + H]^+$ calcd = 1411.7, found = 1412). Cyclization of 4 mg of **17-x** (2.8 μmol) and purification as described above afforded 2.5 mg of **17** (1.8 μmol, 64%). ^{1}H NMR (400 MHz, 293 K, $CDCl_3$, major conformer only): **L-Phe¹**, N−H (7.63, d, J = 4.9 Hz), $C^{\alpha}H$ (4.53, m), $C^{\beta}H_2$ (3.09, 3.18, m), $C^{\delta,\epsilon,\xi}H$ (7.15−7.31, m); **D-^{Me}N-Ala²**, N−CH_3 (2.36, s), $C^{\alpha}H$ (5.50, br), $C^{\beta}H_3$ (1.17, d, J = 7.0 Hz). ESI-MS: $[M + H]^+$ calcd = 1393.7, found = 1394.

***cyclo*[(-L-^{Me}N-Phe¹-D-Ala²)₄-] (18).** Linear octapeptide (-L-^{Me}N-Phe-D-Ala)$_4$ (**18-x**) was synthesized on *N*-Boc-D-Ala-(OCH$_2$)-Pam resin and cleaved with HF to give the desired product as its TFA salt after purification by RP-HPLC (ESI-MS, $[M + H]^+$ calcd = 947.5, found = 947). Cyclization of 103 mg of **18-x** (97 μmol) and purification as described above afforded 44 mg of **18** (47 μmol, 49%). ^{1}H NMR (500 MHz, 293 K, $CDCl_3$): **L-^{Me}N-Phe¹**, N−CH_3 (2.87, s), $C^{\alpha}H$ (5.06, br), $C^{\beta}H_2$ (3.03, dd, J = 11.2, 14.3 Hz; 3.26, dd, J = 5.1, 14.5 Hz), $C^{\delta,\epsilon,\xi}H$ (7.13−7.26, m); **D-Ala²**, N−H (7.03, d, J = 5.0 Hz), $C^{\alpha}H$ (4.61, br), $C^{\beta}H_3$ (0.86, d, J = 6.4 Hz). IR (293 K, 1 mM, $CHCl_3$): 3343, 3399 (amide A); 1644, 1675 (amide $I_{\perp}$). ESI-MS: $[M + H]^+$ calcd = 929.5, found = 930.

***cyclo*[(-L-Phe¹-Aib²)₄-] (19).** Octapeptide (L-Phe¹-Aib²)$_4$ (**19-x**) was synthesized *N*-Boc-L-Phe-(OCH$_2$)-Pam resin (0.68 mmol scale). HF cleavage and purification by RP-HPLC gave 305 mg of the desired product as its TFA salt (288 μmol, 42%; ESI-MS, $[M + H]^+$ calcd = 947.5, found = 948). Subjection of 305 mg of **19-x** (288 μmol) to standard cyclization and purification conditions (*vide supra*) afforded 203 mg of the cyclic octapeptide **19** (219 μmol, 76%). ^{1}H NMR (500 MHz, 318 K, $CDCl_3$, major conformer only): **L-Phe¹**, N−H (7.11, br), $C^{\alpha}H$ (4.42, br), $C^{\beta}H_2$ (3.27, 3.45, m), $C^{\delta,\epsilon,\xi}H$ (7.11−7.25, m); **Aib²**, N−H (7.17, br), $C^{\beta 1,\beta 2}H_3$ (1.26, 1.30, br s). IR (293 K, 1 mM, $CHCl_3$): 3269, 3379 (amide A); 1676 (amide $I_{\perp}$); 1520 (amide $II_{||}$). ESI-MS: $[M + H]^+$ calcd = 929.5, found = 930.

***cyclo*[(-D-α-Me-Phe¹-L-Ala²)₄-] (20).** Linear octapeptide (-D-α-Me-Phe¹-L-Ala²)$_4$ (**20-x**) was synthesized on *N*-Boc-L-Ala-(OCH$_2$)-Pam resin (0.25 mmol scale) as above but using HATU as activating agent.[44b−d] HF cleavage and purification by RP-HPLC gave 222 mg of the desired product as its TFA salt (210 μmol, 84%; ESI-MS, $[M + H]^+$ calcd = 947.5, found = 947). Subjection of 101 mg of **20-x** (95 μmol) to standard cyclization and purification conditions (*vide supra*) afforded 59 mg of the cyclic octapeptide **20** (64 μmol, 67%). ^{1}H NMR (500 MHz, 323 K, $CDCl_3$): **D-α-Me-Phe¹**, N−H (7.36, br), $C^{\beta 1}H_2$ (3.31, d, J = 13.6 Hz; 3.09, d, J = 13.6 Hz), $C^{\beta 2}H_3$ (1.38, s), $C^{\delta,\epsilon,\xi}H$ (7.18−7.30, m); **L-Ala²**, N−H (7.08, br), $C^{\alpha}H$ (4.27), $C^{\beta}H_3$ (1.43, d, J = 7.4 Hz). IR (293 K, 1 mM, $CHCl_3$): 3277, 3369 (amide A); 1674 (amide $I_{\perp}$); 1518 (amide $II_{||}$). ESI-MS: $[M + H]^+$ calcd = 929.5, found = 929.

^{1}H NMR Assignments of Cyclic Peptides 1−20. ^{1}H NMR spectra ($CDCl_3$) of all entries in Table 1 were assigned from the corresponding double-quantum-filtered 2D COSY (2QF-COSY)[14] and/or ROESY[15] spectra acquired at the concentration and temperature indicated. Mixing times (~300 ms) were not optimized for ROESY experiments; consequently, of the twofold symmetrical dimer-forming peptides examined, only **4**, **5**, **7**, and **11** displayed expected cross-strand $d_{\alpha-\alpha}$ ROEs (Figures 6 and 7). Therefore, dimeric species **d** and **d*** in ^{1}H NMR spectra of **8** were assigned by analogy to ROESY spectra of **7**, while the ROESY spectrum of **11** was used to differentiate **d** and **d*** for **9**, **10**, and **12** (Table 1). Due to conformational averaging on the NMR time scale, peptides with C_n sequence symmetry (n = 2, 4) generally display C_n symmetrical ^{1}H NMR spectra for monomeric species and D_n symmetrical spectra for dimeric species. Spectra were typically acquired using Bruker's standard pulse sequence on an AMX-400 or 500-MHz spectrometer as indicated for each peptide and referenced to residual $CHCl_3$ solvent peaks (δ = 7.24). Data were processed using the FELIX software package (Molecular Simulations, Inc.).

Measurement of Solution Association Constants by Variable-Concentration ^{1}H NMR. Solution dimerization experiments were

typically carried out as indicated in the following representative procedure for peptide **12**: 50 mg of HPLC-purified peptide was dissolved in 2 mL of freshly distilled, deoxygenated $CDCl_3$ and dried for 0.5 h over activated powdered 4-Å molecular sieves. The suspension was filtered through a fine-porosity fritted glass funnel using N_2 pressure, and the following NMR samples were prepared by diluting the indicated aliquot of anhydrous peptide stock solution to 500-μL total volume with dry, degassed $CDCl_3$: *a*, 100; *b*, 200; *c*, 300; *d*, 400; and *e*, 500 μL. After acquiring the 1D ^{1}H NMR spectrum of each sample (500 MHz, 293 K), 50 μL of 0.1% dioxane in dry degassed $CDCl_3$ was added to sample *d* as an internal concentration standard to give sample *f*. The 1D ^{1}H NMR spectrum of *f* was then acquired, and from the integral ratio of dioxane to total (Ala *N*-CH_3 + Phe $C^{\beta}H_2$), the concentration of the stock solution was determined to be 38.1 mM. For spectra *a*−*e*, the integral ratio (Ala dimer $C^{\alpha}H$)/[(Ala dimer $C^{\alpha}H$) + 2(Val monomer $C^{\alpha}H$)] was measured and plotted as the dependent variable vs total peptide concentration, followed by nonlinear curve fitting with eq 1 to give $K_a = 12$ M^{-1}.

van't Hoff Analysis of Dimerization by Parent Peptide 1. Cyclic peptide **1** was dissolved at a concentration of 1.03 mM in dry $CDCl_3$ (no molecular sieves). 1D ^{1}H NMR spectra of the resulting sample were acquired at intervals of 10 K in the temperature range 273−323 K. Single-point determinations of K_a were made at each temperature by measuring the ratio of integral intensity for monomer and dimer. A plot was then made of $1/T$ (K) vs ln K_a, from which were established the following thermodynamic parameters for the dimerization of **1**: $\Delta C_p = -203.1$ cal K^{-1} mol^{-1}, $\Delta H°_{298} = -11.0$ kcal mol^{-1}, and $\Delta S°_{298} = -23.7$ cal K^{-1} mol^{-1}.

Solution FT-IR Characterization of Selected Cyclic Peptides. Lyopholized peptide was dissolved at 1−4 mM in $CHCl_3$ and placed in a CaF_2 solution IR cell. Spectra were acquired in transmission mode using a Nicolet Magna-IR 550 spectrometer with a step size of 4 cm^{-1}.

ESI Mass Spectrometry. ESI-MS experiments were performed on an API III Perkin-Elmer SCIEX triple-quadrupole mass spectrometer. Samples were typically introduced into the mass analyzer at a rate of 4.0 mL/min. The declustering potential was maintained between 50 and 200 V, while the emitter voltage was typically maintained at 4000 V. For dimerization experiments, peptide **1** was dissolved at ∼100 μM in 98:1:1 (v/v/v) $CHCl_3$/AcOH/MeOH.

Preparation of Peptide Single Crystals for X-ray Analysis. In a typical experiment, 3 mg of HPLC-purified peptide was dissolved in 1 mL of CH_2Cl_2 and equilibrated via vapor-phase diffusion against 5 mL of hexanes, resulting in spontaneous crystallization after 2−4 days. The mother liquor was then drawn off, and, if necessary, the sample was recrystallized as before. Single crystals were flame sealed in high-quality crystallographic capillary tubes to guard against sample degradation during data acquisition.

X-ray Crystallographic Analysis of Peptides 1, 2, 3, and 9. Data were collected on a Rigaku AFC6R diffractometer equipped with a rotating copper anode (Cu Kα) and a highly ordered graphite monochromator. All calculations were performed on a Silicon Graphics Personal Iris 4D/35 and an IBM-compatible PC using the programs TEXSAN (Molecular Structure Corp., The Woodlands, TX 77381), SHELX-97 (G. M. Sheldrick, Institute für Anorganische Chemie, Universitat Gottingen, D-37077 Göttingen, Germany), and SHELX-PC (G. M. Sheldrick, Siemens Analytical X-ray Instruments Inc., Madison, WI.) Crystallographic parameters are available in the Supporting Information.

Acknowledgment. We thank Raj Chadha for X-ray crystallographic analysis of **1**, **2**, **3**, and **9**; Brian Bothner for conducting ESI-MS studies with **1**; and Mallika Sastry, Jay Siegel (UCSD), and Alan Kennan for helpful discussions. This work was supported by the Office of Naval Research (N00014-94-1-0365) and the National Institutes of Health (GM 52190). J.M.B. and K.K. acknowledge NSERC of Canada and the Ministry of Education, Science, and Culture of Japan, respectively, for postdoctoral fellowship support. T.D.C. is the recipient of an NSF predoctoral fellowship.

Supporting Information Available: Tables of crystal data and structure refinement, atomic coordinates and equivalent isotropic displacement coefficients, bond lengths and angles, anisotropic displacement coefficients, and hydrogen atom coordinates and isotropic displacement coordinates, ORTEP drawings with atom labels, and unit cell views of **1**, **2**, **3**, and **9** (39 pages, print/PDF). See any current masthead page for ordering information and Web access instructions.

JA981485I